

# **Design optimization of a nose profile for a canard configuration missile**

**AN ANALYSIS PROJECT**

Submitted by:

Kartikeya Akojwar

Under the guidance of:

Aman Sharma

Dr. Rajesh Gupta

Rishi Dhar

Hrushikesh Varwadear

## Contents

Declaration:.....	5
Acknowledgement: .....	6
Introduction: .....	7
Current analysis techniques:.....	8
Research Question:.....	9
Summary of proposal:.....	10
Preliminary Data:.....	11
Evidence of Importance:.....	11
Important categories and relationships:.....	12
Tail Control:.....	14
Canard Control:.....	15
Wing Control:.....	17
Unconventional Control:.....	18
Unconventional control technologies: .....	18
Preliminary findings: .....	19
Literature Survey:.....	21
Methodology: .....	25
MODEL CREATION USING SOLIDWORKS:.....	25
Control Volume Sizing:.....	26
Missile Design and Drawing:.....	27
Missile model drawing steps in solidworks:.....	27
A. IMPORT OF MODELS INTO DESIGNMODELER .....	51
1. Meshing.....	53
2. Common Mesh Settings .....	54
3. Inflation Settings.....	55

4.	Mesh Quality .....	55
B.	SETUP OF CFX-PRE (SETUP) .....	56
1.	General Setup.....	56
2.	Assignment of Boundaries .....	58
3.	Parameters Setup .....	58
a.	Analysis Type and Material Setup .....	58
b.	Inlet Setup.....	59
c.	Outlet Setup.....	60
d.	Opening Setup .....	60
e.	Symmetry Setup.....	61
f.	Solver Control Setup .....	61
g.	Expert Parameters .....	62
C.	OBTAINING SOLUTIONS FROM CFX.....	63
1.	Starting the CFX-Solver Manager .....	63
2.	Partitioning the Problem.....	63
3.	Display Monitors.....	63
4.	Displaying Simulation Results .....	65
a.	Flow Field Display .....	65
b.	Function Calculator.....	66
	The Project: .....	0
	Introduction: .....	0
A.	CURRENT ANALYSIS TECHNIQUES .....	0
B.	OVERVIEW OF SOLIDWORKS modelling.....	1
1.	Model Selection .....	2
2.	Assumptions Made for the Model .....	3
a.	<i>Exclusion of Missile Hangers</i> .....	5

<i>b.</i>	<i>Inclusion of a Hinge to Hold Canards to Body</i> .....	5
<i>c.</i>	<i>Seating of the Tail Wings</i> .....	5
<i>d.</i>	<i>Shape of the Wings and Canards</i> .....	6
<i>e.</i>	<i>Accuracy of Dimension Given in [1] and [2]</i> . ....	6
C.	OVERVIEW OF ANSYS CFX.....	6
FUTURE SCOPE:.....		8
Results and Discussions: .....		11
Conclusions and summary: .....		18
REFERENCES .....		19

## Declaration:

We hereby declare that the project work entitled "**Study of nozzle parameters on jet impingement for efficient heat transfer techniques**" submitted to Maulana Azad National Institute of technology as a record of an original work done by us under the guidance of **Dr. Rajesh Gupta**, Associate Professor, Department of Mechanical Engineering, MANIT Bhopal; and this project work is submitted in the partial fulfillment of the requirements for the minor project to be submitted for the sixth semester of our study. The results embodied in this project report have not been submitted to any other institute or at any conference.

And we further declare that to our knowledge, the structure and content of this project are fully original and has not been submitted before for any purpose.

Submitted by:

Name	Scholar Number	Signature
Kartikeya Akojwar	131116109	
Aman Singh	131116045	
Hrushikesh V.	131116234	
Rishi Dhar	131116032	

Under the guidance of:

Dr. Rajesh Gupta

Associate professor,

Dept. Of Mechanical Engineering,

MANIT Bhopal

## Acknowledgement:

Perseverance, inspiration and motivation has always played a key role in any venture. It is not just brain that matters the most, but what which guides them. The character, the heart, the generous qualities and progressive forces. What was conceived just as an idea materialized slowly into concrete facts. The metamorphosis took endless hours of toil, had its moment of frustration, but in the end everything seemed to have sense”.

At this level of understanding it is often difficult to understand a wide spectrum of knowledge without proper guidance and advice. Hence, we take this opportunity to express our heartfelt gratitude to our project guide **Dr. Rajesh Gupta** who had faith on us and allowed us to work on this project. We would like to thank Prof. J.L Bhagoria (HOD MECHANICAL)for his immense interest, valuable guidance and constant source of inspiration and kind co-operation through the period of word undertaken, which has been instrumented in the success of our project.

We would also like to acknowledge our profound sense of gratitude to all the teachers who have been instrumental for providing us technical knowledge and moral support to complete the project with full understanding.

Hrushikesh Varawdekar

Rishi Dhar

Aman Singh

Kartikeya Akojwar

## Introduction:

A Missile is defined as a space-traversing unmanned vehicle that contains the means for controlling its flight path. A guided missile is considered to operate only above the surface of the Earth, so guided torpedoes do not meet the above definition. Missiles are classified by the physical areas of launching and the physical areas containing the target. The four general categories of guided missiles are: surface-to-surface; surface-to-air; and air-to-air.

The earliest form of a missile was probably a rock, which, when hurled through the air, would follow a curved ballistic path. The early 1900's, the development of guided missiles was begun. Significant advances in missile technology were made by German scientists, during World War II. The dispersion of these advances to other countries following the war resulted in accelerating the development of guided missiles. In the late 1940's and early 1950's there was a proliferation in the development of missile systems in many countries. These developments were based primarily on experimental work and on relatively crude analytical techniques.

The R.A.F. produced 6 graceful monoplanes with aerials fitted chord-wise on the wing and on the aft body. The weapons were launched from a lorry with a compressed air catapult which, in itself, was an idea ahead of its time.

Much of the early missile development was clearly facilitated by the German influence; much was developed from test flight; and some was backed by wind tunnel programs such as the APL/NOL Bumblebee program. Missile research within NACA was nebulous at best in the late 1940's. At about that time, however, and into the 1950's many missile research programs were undertaken at both the Langley and the Ames research centers of NACA/NASA. Most of the effort was expanded in experimental wind-tunnel investigations and some in free-flight rocket-model tests. In the 1950's, some analytical and semi empirical estimating techniques were being developed for use with missile concepts. Some of this work that should be mentioned was produced by a team of researchers at NACA-Ames that included Jack Nielsen. In 1960's the procedures developed were reasonably useful for design purposes but were somewhat time consuming. In addition, for best results, the procedures often

required the use of empirical correlation factors. These factors generally came from experimental test data which, in effect, resulted in an increase in the amount of test data being obtained from generalized research models rather than from tests of specific configurations. Even so, experimental data was generally required when detailed results were required or when regimes such as high angles of attack were to be explored or regions of combined pitch and roll.

The prediction of aerodynamic coefficients is essential in assessing the performance of new designs including different nose configurations. Accurate determination of aerodynamics is critical to the low-cost development of new advanced guided projectiles, rockets, missiles, and smart munitions. Fins, canards, and jets can be used to provide control for maneuvering projectiles and missiles. This study uses Computational Fluid Dynamics code, ANSYS-CFX to predict the static aerodynamic characteristics of a canard-wing missile configuration with a parabolic nose, triangular wedge canards and fixed trapezoidal wings. The study was conducted for Mach numbers 0.2, 0.8 and 1.2. The results have been compared against data from a semi-empirical method for a hemispherical nose missile.

Apart from Wind-Tunnel testing, Ansys as a software has been continually used for design optimization and process simulation.

## CURRENT ANALYSIS TECHNIQUES:

The use of computers to solve the Navier-Stokes equations was a major breakthrough for the study of aerodynamic problems. Before this, engineers and researchers were left with only using actual wind tunnel tests and approximations to determine the aerodynamic characteristics of flight objects. Currently, there are three primary methods that can be used for the study of flight vehicles. The most obvious and time honored is the use of a wind tunnel and an actual model of the vehicle to be tested. This would yield the most accurate aerodynamic characteristics of the vehicle. The second method uses software that contains a database of wind tunnel tests and other analytical data to predict the aerodynamic characteristics of the flight vehicle. An example of such a program is Aeroprediction 2009 (APo9). The third method is to use Computational Fluid Dynamics (CFD) codes that solve the Navier-Stokes

equations. Examples of such programs include NASA's OVERFLOW and commercially available codes like ANSYS-CFX.

## RESEARCH QUESTION:

The development of missiles have long been studied by aerodynamicists and the advancements in the missile design has resulted in tremendous evolution. Missile design optimization has seen elaboration of a blend of parameters which include the structural, aerodynamic, flight operational, body design, etc. among which nose profile optimization has proven to be the most successful development in the history of missile design advancement.

The research question involved in the present study is to study and analyze various nose profiles and conclude their performance characteristics. The nose profiles studied here were hemispherical, ellipsoids with different eccentricities and parabolic. The most significant development in the history of missile design advancement was the changeover from the usual sharp nose profile to blunt edged profiles. The most common missile nose profile that is now in application is the ogive nose profiles but the study here is based on the common geometrical curves like hemisphere, ellipse and parabola all of which have a smooth edged boundaries. This thesis gives a complete insight about the procedure adopted in conducting a simulation of fluid flow around a specific missile profile with a particular nose design, Mach number of the fluid flow domain and angle of attack.

The gradual development of the research was from conducting a complete analysis of a missile with a hemispherical nose profile to validate the simulation model for the CFD analysis conducted on the missile. The analysis model validation was basically to compare the k-epsilon and Shear Stress Transport model to conclude that SST is better than k-epsilon. The next comparison was made between a parabolic and a hemispherical nose profile to compare the various fluid domain characteristics like the temperature, pressure, Mach number, velocity, etc. To further the research involved, the nose profile designs in between the hemispherical and parabolic nose profiles were taken and analyzed. The geometrical shaped in between hemispheres and parabolas are ellipses defined by particular eccentricities. The ellipsoids of eccentricities

0.2, 0.4, 0.6 and 0.8 were taken for analysis and comparison of performance parameters was done.

This study used the Computational Fluid Dynamics code, ANSYS-CFX to predict the static aerodynamic characteristics of a canard-wing missile configuration with a hemispherical nose, triangular wedge canards and fixed trapezoidal wings. The study was conducted for Mach numbers of 0.2, 0.8 and 1.2. The results were compared against experimental data from actual wind tunnel tests and data from a semi-empirical method, APo9. The ANSYS-CFX results showed good agreement for  $C_N$ ,  $C_M$ , and  $C_L$  but less agreement for  $C_A$  when compared to the experimental results.

## SUMMARY OF PROPOSAL:

The study used the Computational Fluid Dynamics code, ANSYS-CFX to predict the static aerodynamic characteristics of a canard-wing missile configuration with a hemispherical nose, triangular wedge canards and fixed trapezoidal wings. The study was conducted for Mach numbers of 0.2, 0.8 and 1.2. The results were compared against experimental data from actual wind tunnel tests and data from a semi-empirical method, APo9. The ANSYS-CFX results showed good agreement for  $C_N$ ,  $C_M$ , and  $C_L$  but less agreement for  $C_A$  when compared to the experimental results.

The use of computers to solve the Navier-Stokes equations was a major breakthrough for the study of aerodynamic problems. Before this, engineers and researchers were left with only using actual wind tunnel tests and approximations to determine the aerodynamic characteristics of flight objects. Currently, there are three primary methods that can be used for the study of flight vehicles. The most obvious and time honored is the use of a wind tunnel and an actual model of the vehicle to be tested. This would yield the most accurate aerodynamic characteristics of the vehicle. The second method uses software that contains a database of wind tunnel tests and other analytical data to predict the aerodynamic characteristics of the flight vehicle. An example of such a program is Aeroprediction 2009 (APo9). The third method is to use Computational Fluid Dynamics (CFD) codes that solve the Navier-Stokes

equations. Examples of such programs include NASA's OVERFLOW and commercially available codes like ANSYS-CFX.

## Preliminary Data:

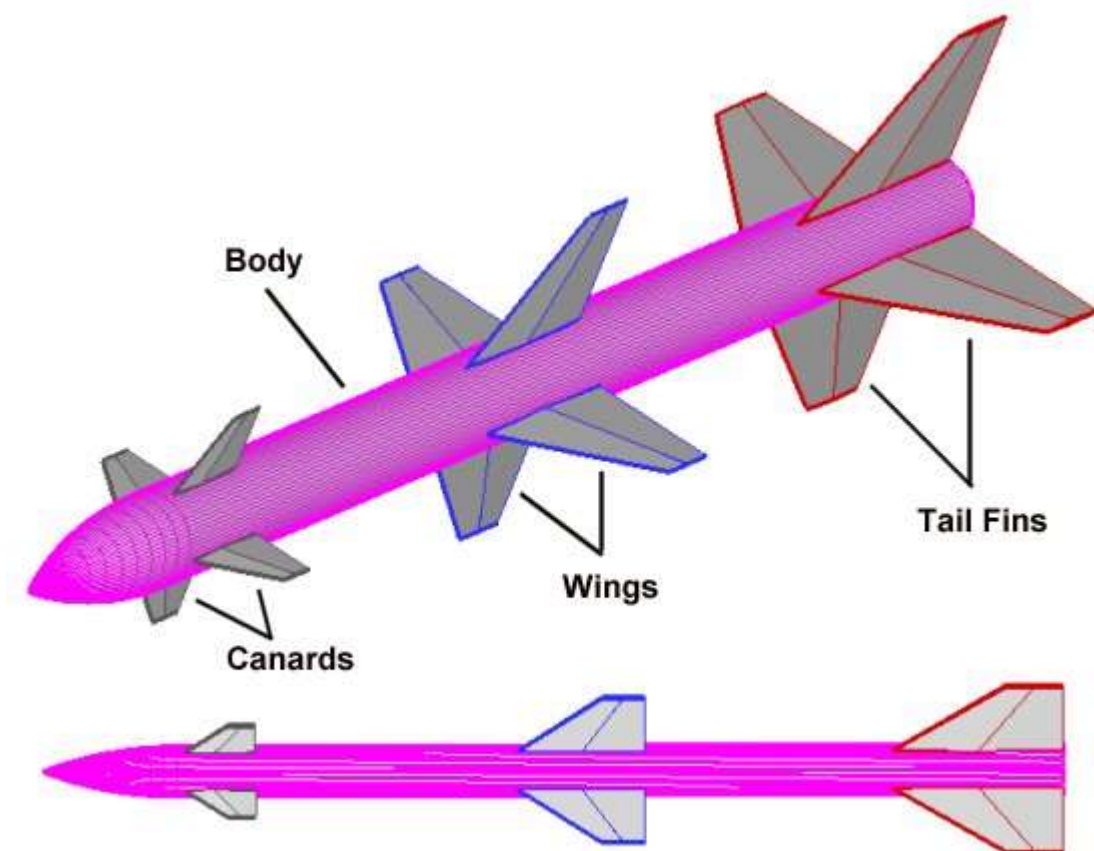
### EVIDENCE OF IMPORTANCE:

The development of missiles have long been studied by aerodynamicists and the advancements in the missile design has resulted in tremendous evolution. Missile design optimization has seen elaboration of a blend of parameters which include the structural, aerodynamic, flight operational, body design, etc. among which nose profile optimization has proven to be the most successful development in the history of missile design advancement. The most importance breakthrough in aerodynamics is transition of nose profile from sharp to blunt. We further selected nose profiles of different geometries and performed CFD analysis. We compared the performance of missile having different nose profiles at different angle of attack. From different contours and plots (temperature, total pressure, Mach of fluid domain) we have obtained after analysis, we compared the performance of missile for different nose profiles. We also calculated aerodynamic coefficients  $C_a$ ,  $C_n$ ,  $C_m$  to get the required analysis results and compare the results.

The heart of a missile is the body, equivalent to the fuselage of an aircraft. The missile body contains the guidance and control system, warhead, and propulsion system. Some missiles may consist of only the body alone, but most have additional surfaces to generate lift and provide maneuverability. Depending on what source you look at, these surfaces can go by many names. In particular, many use the generic term "fin" to refer to any aerodynamic surface on a missile. Missile designers, however, are more precise in their naming methodology and generally consider these surfaces to fall into three major categories: canards, wings, and tail fins.

The example shown above illustrates a generic missile configuration equipped with all three surfaces. Often times, the terms canard, wing, and fin are used interchangeably, which can get rather confusing. These surfaces

behave in fundamentally different ways, however, based upon where they are located with respect to the missile center of gravity. In general, a wing is a relatively large surface that is located near the center of gravity while a canard is a surface near the missile nose and a tail fin is a surface near the aft end of the missile.



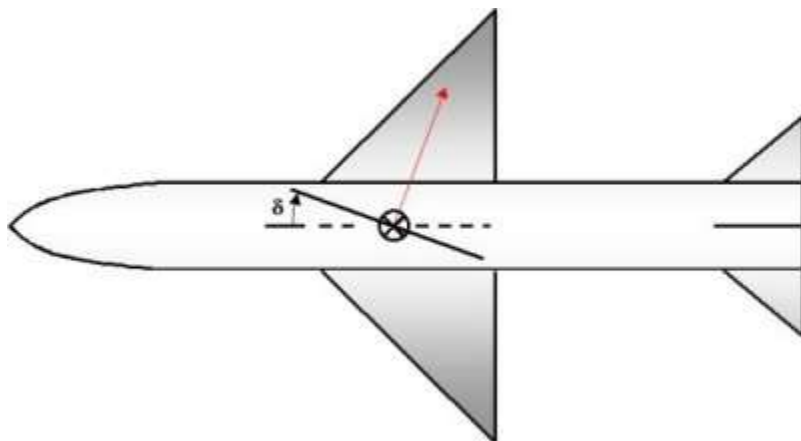
*Major components of a missile*

## IMPORTANT CATEGORIES AND RELATIONSHIPS:

Most missiles are equipped with at least one set of aerodynamic surfaces, especially tail fins since these surfaces provide stability in flight. The majority of missiles are also equipped with a second set of surfaces to provide additional lift or improved control. Very few designs are equipped with all three sets of surfaces.

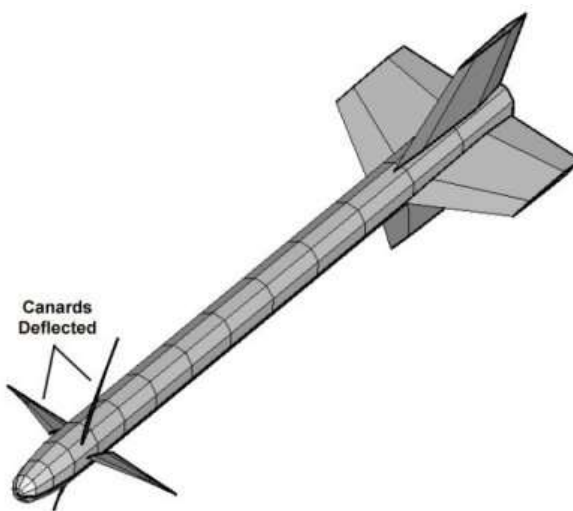
We have discussed how aircraft use control surfaces to turn the plane in different directions in a number of previous questions. Whereas most aircraft

have fixed horizontal and vertical tails with smaller movable rudder and elevator surfaces, missiles typically use all-moving surfaces, like those illustrated below, to accomplish the same purpose.



**Deflection of a control surface on a missile**

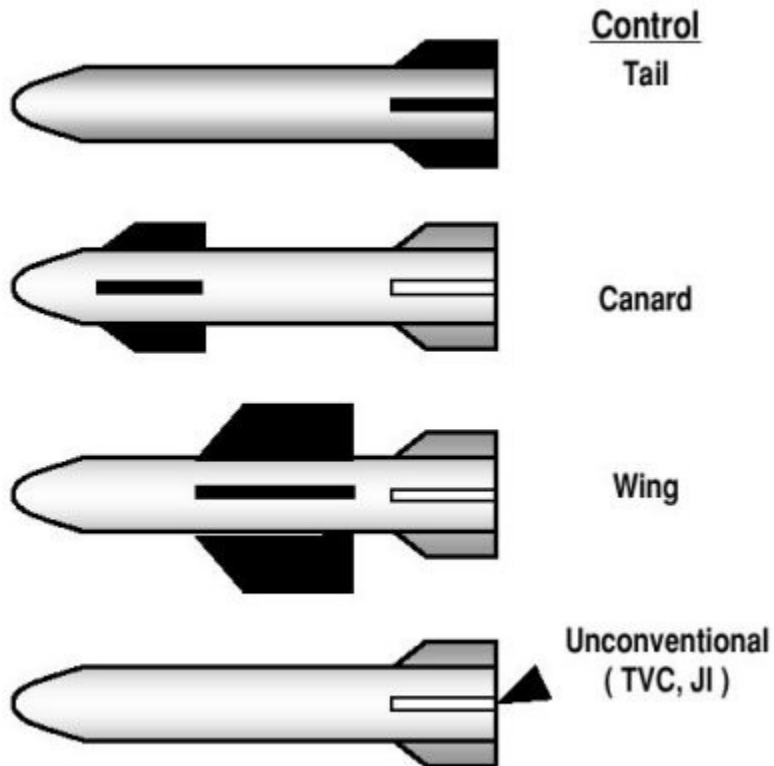
In order to turn the missile during flight, at least one set of aerodynamic surfaces is designed to rotate about a center pivot point. In so doing, the angle of attack of the fin is changed so that the lift force acting on it changes. The changes in the direction and magnitude of the forces acting on the missile cause it to move in a different direction and allow the vehicle to maneuver along its path and guide itself towards its intended target. An example of a control surface deflection on an AIM-9M Sidewinder model is illustrated below.



**Canard deflections on an AIM-9M Sidewinder**

Canards, wings, and tails are often lumped together and referred to as aerodynamic controls. A more recent development in missile maneuvering systems is called unconventional control. Most unconventional control systems involve some form of thrust vector control (TVC) or jet interaction (JI).

We have now introduced four major categories of missile flight control systems--tail control, canard control, wing control, and unconventional control--so let's briefly take a closer look at each type.



#### **Four main categories of missile flight controls**

##### **Tail Control:**

Tail control is probably the most commonly used form of missile control, particularly for longer range air-to-air missiles like AMRAAM and surface-to-air missiles like Patriot and Roland. The primary reason for this application is because tail control provides excellent maneuverability at the high angles of attack often needed to intercept a highly maneuverable aircraft. Missiles using tail control are also often fitted with a non-movable wing to provide additional lift and improve range. Some good examples of such missiles are air-to-ground

weapons like Maverick and AS.30. Tail control missiles rarely have canards, although one such example is AIM-9X Sidewinder. A selection of 23 representative missiles using tail control is pictured below.



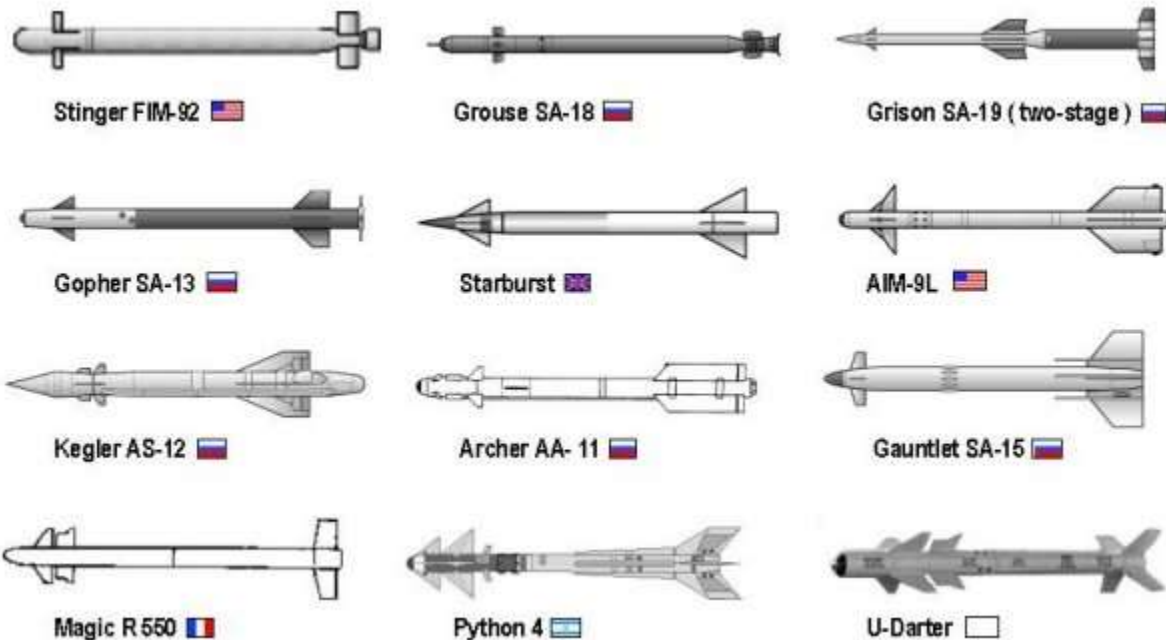
### Missiles with tail control

#### Canard Control:

Canard control is also quite commonly used, especially on short-range air-to-air missiles like AIM-9M Sidewinder. The primary advantage of canard control is better maneuverability at low angles of attack, but canards tend to become ineffective at high angles of attack because of flow separation that causes the surfaces to stall. Since canards are ahead of the center of gravity, they cause a destabilizing effect and require large fixed tails to keep the missile stable. These two sets of fins usually provide sufficient lift to make wings unnecessary. Shown below are twelve examples of canard control missiles.

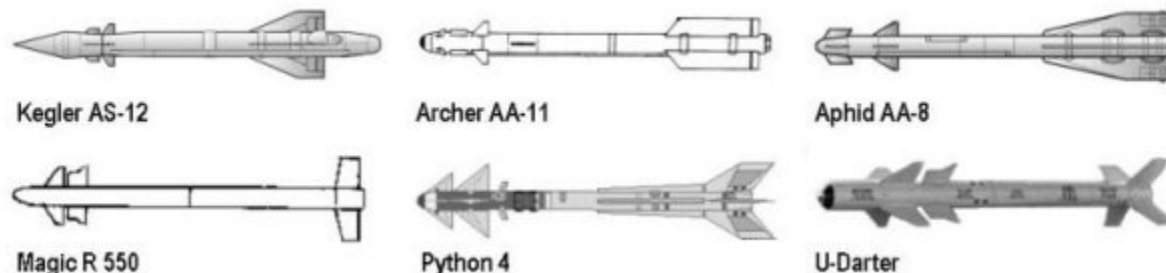
A further subset of canard control missiles is the split canard. Split canards are a relatively new development that has found application on the latest generation of short-range air-to-air missiles like Python 4 and the Russian

AA-11. The term split canard refers to the fact that the missile has two sets of canards in close proximity, usually one immediately behind the other. The first canard is fixed while the second set is movable.



### Missiles with canard control

The advantage of this arrangement is that the first set of canards generates strong, energetic vortices that increase the speed of the airflow over the second set of canards making them more effective. In addition, the vortices delay flow separation and allow the canards to reach higher angles of attack before stalling. This high angle of attack performance gives the missile much greater maneuverability compared to a missile with single canard control. Six examples of split canard missiles are shown below.

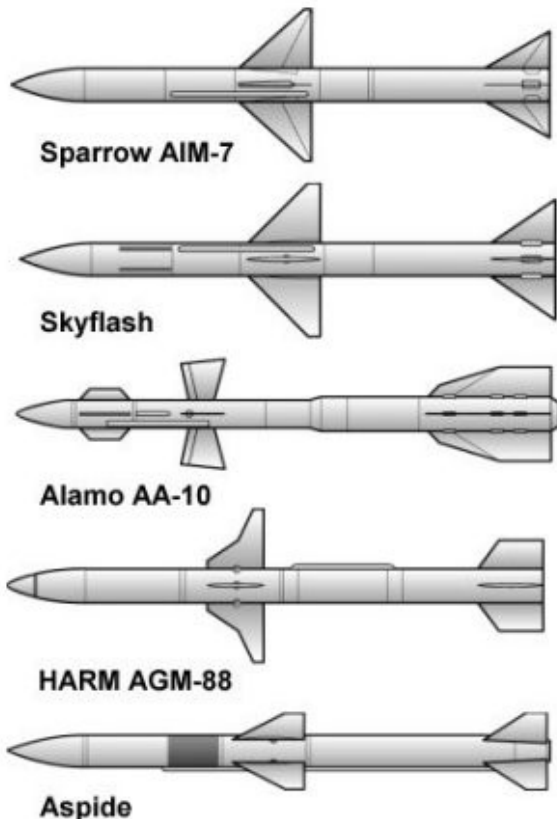


### Missiles with split canard control

Many smart bombs also use canard control systems. Most notable of these are laser guided bombs such as the Pave way series.

### **Wing Control:**

Wing control was one of the earliest forms of missile control developed, but it is becoming less commonly used on today's designs. Most missiles using wing control are longer-range missiles like Sparrow, Sea Skua, and HARM. The primary advantage of wing control is that the deflections of the wings produce a very fast response with little motion of the body. This feature results in small seeker tracking error and allows the missile to remain locked on target even during large maneuvers. The major disadvantage is that the wings must usually be quite large in order to generate both sufficient lift and control effectiveness, which makes the missiles rather large overall. In addition, the wings generate strong vortices that may adversely interact with the tails causing the missile to roll. This behavior is known as induced roll, and if the effect is strong enough, the control system may not be able to compensate. A few examples of wing control missiles are shown below.



### **Missiles with wing control**

#### **Unconventional Control:**

Unconventional control systems is a broad category that includes a number of advanced technologies. Most techniques involve some kind of thrust vectoring. Thrust vectoring is defined as a method of deflecting the missile exhaust to generate a component of thrust in a vertical and/or horizontal direction. This additional force points the nose in a new direction causing the missile to turn. Another technique that is just starting to be introduced is called reaction jets. Reaction jets are usually small ports in the surface of a missile that create a jet exhaust perpendicular to the vehicle surface and produce an effect similar to thrust vectoring.

#### **Unconventional control technologies:**

These techniques are most often applied to high off-boresight air-to-air missiles like AIM-9X Sidewinder and IRIS-T to provide exceptional maneuverability. The greatest advantage of such controls is that they can function at very low

speeds or in a vacuum where there is little or no airflow to act on conventional fins. The primary drawback, however, is that they will not function once the fuel supply is exhausted.

#### ◆ Jet Vane + Aero Control



**Archer AA-11**



**Mica**



**Sea Sparrow RIM-7**



**AIM-9X**



**Sea Wolf GWS 26**



**IRIS-T**

#### ◆ Reaction Jet + Aero Control



**PAC-3**



**Aster FSAF 15**

#### ◆ Movable Nozzle + Aero Control



**Standard Missile RIM-66/67**

#### ◆ Movable Nozzle + Reaction Jet



**THAAD**

#### ◆ Reaction Jet



**LOSAT**

### Missiles with unconventional controls

Examples of missiles employing unconventional controls are shown above. Note that most missiles equipped with unconventional controls do not rely on these controls alone for maneuverability, but only as a supplement to aerodynamic surfaces like canards and tail fins.

## PRELIMINARY FINDINGS:

Coefficient of Axial Force:

Ca or Coefficient of Axial Force signifies the ratio of Axial Force to the Kinetic Energy of Air while propulsion. It is a very important for Principle Drag calculation and is best when near unity.

The formula for Ca is =  $\frac{F_x}{\frac{1}{2} \rho A^2}$

Coefficient of Normal Force:

C<sub>n</sub> or Coeffiecient of Normal Force is defined as the ratio of Normal Force experienced by the Missile Body to that of Kinetic Energy due to vertical component of velocity. It must such that the Lateral acceleration remains undisturbed.

The formula is =  $\frac{F_y}{\frac{1}{2}\rho AV^2}$

Coefficient of Moment

C<sub>m</sub> is the turning moment about the Centre of Mass of the Missile. It is the ratio of Torque about the axis which is perpendicular to the plane to the Torque due to the Velocity at Tail.

Its formula is  $\frac{T}{\frac{1}{2}\rho AL^2}$

### Numerical Method

The external flow around the missle features was fond to be turbulent due to high speeds (more than 65m/s). The complete set of equations which govern the flow can be given by the continuity equation and Navier-Stokes equation with suitable turbulent scheme.

The continuity equation governs the balance of mass across a control volume and is written as

$$\frac{\partial \rho}{\partial t} + \nabla \cdot (\rho u) = 0$$

where,  $\rho$  is the air density,  $t$  is time and  $u$  is the flow velocity vector field.

In addition to continuity equation, all the forces on a control volume are given by the Navier-Stokes equation

$$\frac{\partial(\rho u_i)}{\partial t} + u_j \frac{\partial(\rho u_i)}{\partial x_j} = - \frac{\partial \rho}{\partial x_i} + \frac{\partial}{\partial x_j} \left( \mu_\theta \frac{\partial u_i}{\partial x_j} \right) + \rho F_i ; i = 1,2,3; j = 1,2,3$$

where,  $p$  is the pressure,  $\mu_v$  is the effective dynamic viscosity, and  $F_i$  is the component of the body force per unit mass. Here, the effective viscosity is approximated by the sum of the laminar and turbulent viscosities.

Here, the effective viscosity is approximated by the sum of the laminar and turbulent viscosities. To solve the Navier-Stokes equation the Shear Stress turbulence model was adopted. The model combines the k-omega turbulence model and K-epsilon turbulence model such that the k-omega is used in the inner region of the boundary layer and switches to the k-epsilon in the free shear flow. Authors who use the SST k- $\omega$  model often merit it for its good behavior in adverse pressure gradients and separating flow.

The complete formulation of the SST model as given as

$$\begin{aligned}\frac{\partial(\rho k)}{\partial t} + \frac{\partial(\rho u_j k)}{\partial x_j} &= \rho P - \beta^* \rho \omega k + \frac{\partial}{\partial x_j} \left[ (\mu + \sigma_k \mu_t) \frac{\partial k}{\partial x_j} \right] \\ \frac{\partial(\rho \omega)}{\partial t} + \frac{\partial(\rho u_j \omega)}{\partial x_j} &= \frac{\gamma}{v_t} P - \beta \rho \omega^2 + \frac{\partial}{\partial x_j} \left[ (\mu + \sigma_\omega \mu_t) \frac{\partial \omega}{\partial x_j} \right] \\ P &= \tau_{ij} \frac{\partial u_j}{\partial x_i} \\ \tau_{ij} &= \mu_t \left( 2S_{ij} - \frac{2}{3} \frac{\partial u_k}{\partial x_k} \delta_{ij} \right) - \frac{2}{3} \rho k \delta_{ij} \\ S_{ij} &= \frac{1}{2} \left( \frac{\partial u_i}{\partial x_j} + \frac{\partial u_j}{\partial x_i} \right)\end{aligned}$$

## Literature Survey:

The research for this project has been comprehensive but sources were one than one. From the onset, we have primarily referred to a thesis by Hong Chuan while his tenure in Naval Postgraduate School, thesis named “Aerodynamic Analysis of a Canard-Missile configuration using Ansys-CFX” which has been a pioneering work, which helped in validating our results for hemispherical Nose Profile. The thesis also compares the result with AP-09, which is an Aero-

Prediction Software database, which gets its values from NASA. His study used the Computational Fluid Dynamics code, ANSYS-CFX to predict the static aerodynamic characteristics of a canard-wing missile configuration with a hemispherical nose, triangular wedge canards, and fixed trapezoidal wings. The study was conducted for Mach numbers of 0.2, 0.8 and 1.2 for the different angle of attack. The results were compared against experimental data from actual wind tunnel tests and data from a semi-empirical method, APo9.

Secondly, we referred “CFD Analysis of Various Nose Profiles”, a Thesis by A Sanjay Varma, G Sai Sathyanarayana, Sandeep J, Department of Aeronautical MRCET, Secunderabad. They compared various nose profiles to know performance over existing conventional nose profiles in this paper. The paper objective was to identify the types of nose profiles and its specific aerodynamic characteristics with minimum pressure coefficient and critical Mach number. The scope of their paper is to develop some prototype profiles with outstanding aerodynamic qualities and low cost for use in construction projects for missile increasing their range and effect on the target. The motivation for such a work is caused by a lack of data on aerodynamics for profiles of some nose cones and especially improved aerodynamic qualities that can be used in designing missiles/ rockets. They present problem is analyzed using ANSYS software in the paper. Flow phenomena observed in numerical simulations during Mach 0.8 for different nose cone profiles are highlighted, critical design aspects and performance characteristics of the selected nose cone are presented.

Thirdly, we referred “Effect of Different Nose Profiles on Subsonic Pressure Coefficients” by Ryan J. Felkel, Department of Mechanical and Aerospace Engineering California State University. In the past decade, small sounding rockets have become an important educational tool for college aerospace engineering programs. These sounding rockets typically reach high subsonic Mach numbers leading to apogees around 3 to 4 km. It is inevitable that air must speed up to travel around the body which leads to negative forebody pressure coefficients. This paper focuses on the comparison of different nose shapes having cylindrical afterbodies, and selecting the best with the least speed up. Two issues are considered: First, the adverse pressure gradient existing overall cylindrical afterbodies can lead to the separation of a

vortex pair at an angle of attack that induces rolling moments on the tailfins. Second, if the forebody local Mach number exceeds unity, the flow will decelerate via a shock wave that may also cause a vortex pair to separate at the angle of attack. Shock waves are also associated with the onset of wave drag. The key metric used here is the minimum pressure coefficient at the base of the forebody because it drives both the cylinder pressure gradient and the critical Mach number. Three configurations were analyzed: cone-cylinders, ogive-cylinders, and specially shaped forebody-cylinders optimized for minimum pressure coefficient. The optimum forebody shape was found by a cut-and-try approach for a given fineness ratio. Incompressible pressure coefficients were calculated using Munk Airship Theory assuming zero angles of attack. The Karman-Tsien Correction Factor was used with the minimum pressure coefficient to find the critical Mach number. Results are shown as charts of both minimum pressure coefficient and critical Mach number as functions of fineness ratio. These charts reveal that the minimal pressure coefficient increases almost exponentially as fineness ratio increases. The cone-cylinder results show the greatest speed up compared to the other two nose profiles. Ogive-cylinders generate less speeding up and the optimum shape as the least speeding up. Also, ogive nose profile is not analyzed by us in this thesis but it provided us this key insight which complemented us in completing our thesis effectively.

Fourthly, we used thesis named “Stability and control characteristics at Mach numbers from 0.20 to 4.63 of a cruciform air-to-air missile with triangular canard controls and a trapezoidal wing.” By E. B. Graves, and R. H. Fournier, National Aeronautics and Space Administration, Langley Research Center, Hampton, VA, NASA TM X-3070, July 1974. Investigations have been conducted in the Langley 8-foot transonic pressure tunnel and the Langley Unitary Plan wind tunnel at Mach numbers from 0.20 to 4.63 to determine the stability and control characteristics of a cruciform air-to-air missile with triangular canard controls and a trapezoidal wing. The results indicate that canards are effective in producing pitching moment throughout most of the test angle-of-attack and Mach number range and that the variations of pitching moment with the lift for trim conditions are relatively linear. There is a decrease in canard effectiveness with an increase in angle of attack up to about Mach 2.50 as evidenced by the

beginning of coalescence of the pitching-moment curves. At a Mach number above 2.50, there is an increase in effectiveness at moderate to high angles of attack. Simulated launch straps have little effect on the lift and pitch characteristics but do cause an increase in drag, and this increase in drag induces a rolling moment at a zero roll attitude where the straps cause an asymmetric geometric shape. The canards are not suitable devices for roll control and, at some Mach numbers and roll attitudes, are not effective in producing pure yawing moments.

Fifthly, we referred thesis “The 2002 Version of the NSWC Aeroprediction Code: Part 1 – Summary of New Theoretical Methodology,” by F. G. Moore, T. C. Hymer, C. Downs and L. Y. Moore, Dahlgren Division Naval Surface Warfare Centre, Dahlgren, VA, NSWCDD/TR-01/108, Mar 2002.

A new version of the aeroprediction code (APC), the AP02, has been developed to address the requirements arising from advanced weapon concepts. The AP02 was formed by adding significant new technology and several productivity improvements to the previous version of the APC, the AP98. New technology added included 6 and 8 fin aerodynamics, improved nonlinear aerodynamics, improved pitch damping predictions, improved power-on base drag estimates, the base-bleed effect on base drag estimation, improved axial force of nonaxisymmetric bodies and trailing-edge flap capability. Other improvements and productivity enhancements include an aerodynamic smoother, ballistic and three degree-of-freedom simulation modules as well as refinements for the pre- and post-processor for inputs and outputs of the AP02. Comparison of the predicted aerodynamics of the AP02 to AP98 and experimental data showed the AP02 to be slightly better than the AP98 in most cases that both codes would handle. However, due to the additional new technology incorporated into the AP02, many new options are available in the AP02 that are not available in the AP98. Therefore, the AP02 is more robust and, on average, is slightly more accurate than the AP98 in predicting aerodynamics of weapons.

We also referred “Analysis of New Aerodynamic Design of the Nose Cone Section Using CFD and SPH” by Bogdan-Alexandru BELEGA, Military Technical Academy, Department of Aircraft Integrated Systems and Mechanics, Blvd.

A new nose cones concept that promises a gain in performance over existing conventional nose cones is discussed in their paper. It was shown that significant performance gains result from the adaptation of the exhaust flow to the ambient pressure. For this complex work, it was necessary to collect and study the various nose cone shapes and the equations describing them? The paper objective was to identify the types of nose cones with ejector channels and specific aerodynamic characteristics of different types of nose cones. The scope of this paper is to develop some prototype profiles with outstanding aerodynamic qualities and low cost for use in construction projects for missile increasing their range and effect on the target. The motivation for such a work is caused by a lack of data on aerodynamics for profiles of some nose cones and especially improved aerodynamic qualities that can be used in designing missiles/ rockets. This design method consists of a geometry creation step in which a three-dimensional geometry is generated, a mathematical model presented and a simple flow analysis (FLUENT Simulation from SolidWorks2012 and ANSYS Simulation with SPH for fluid-structure interaction), the step which predicts the air intake mass flow rate. Flow phenomena observed in numerical simulations during different nose cone operations are highlighted, critical design aspects and operation conditions are discussed, and performance characteristics of the selected nose cone are presented.

## Methodology:

### MODEL CREATION USING SOLIDWORKS:

SolidWorks was used to construct the 3D model of the missile and the corresponding control volume. CFX requires that a control volume has to be created around the missile model to be tested. The two drawings are generated as individual parts in SolidWorks and are saved in Parasolid Format (.x\_t). This format was proven to be more robust and error free when performing the import into ANSYS Design Modeler. The two parts are then mated together using

Design Modeler. This method was shown to be more robust than creating a mold of the object to be tested in SolidWorks.

### Control Volume Sizing:

The sizing of the control volume is important to the simulation. If improperly sized, the simulation run may not produce accurate results or may not run at all. It was noted that the optimal sizing of the control volume is between five to ten times the length of the model at the sides and back and at least the length of the model in front of it. In this study, the control volume was five times the model length at the sides and back and one length in the front of the missile model. Figure 7 shows the model of the control volume in SolidWorks. As there is symmetry in the missile model, the control volume chosen only contains half the missile model. This saves time computationally as the flow in the other half is not calculated and is assumed to be symmetrical across the chosen symmetry plane. This assumption is valid for cases where the AOA is small. As the AOA increases, asymmetric flow fields may form and the analysis has to be done with the complete 3D model of the missile and not the half body.

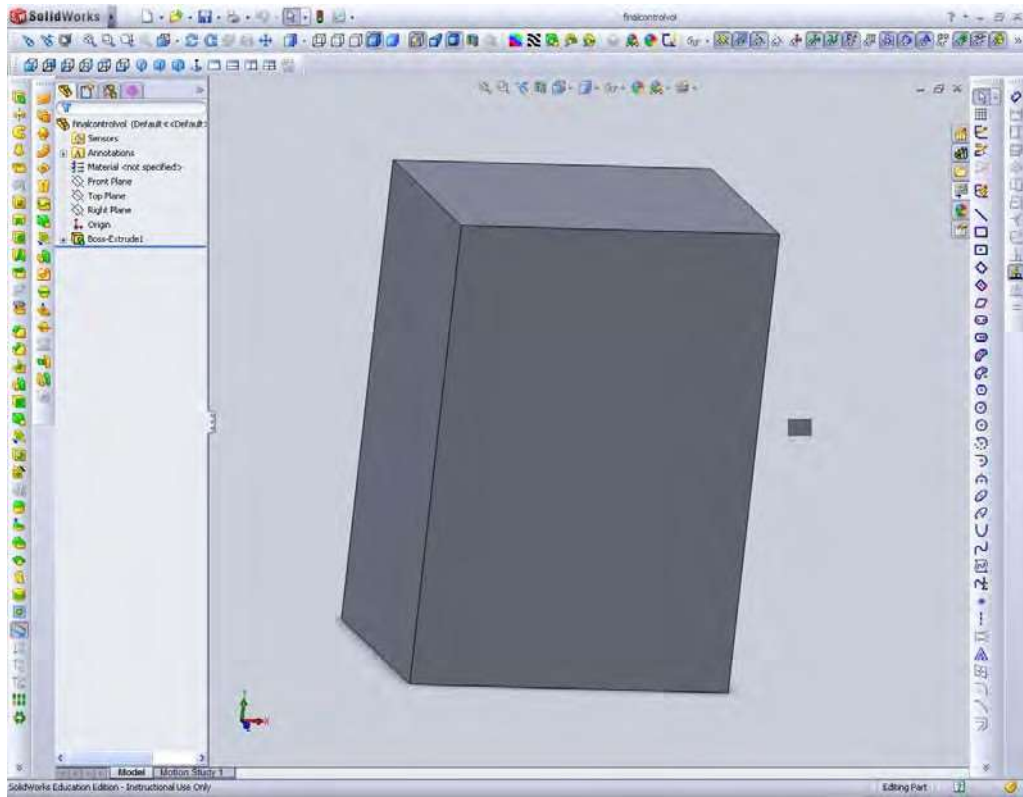
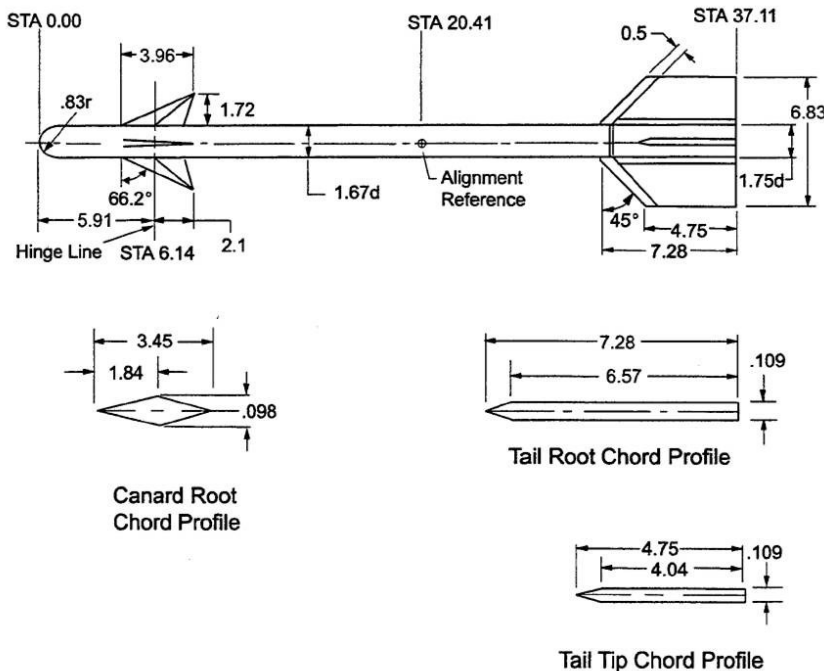


Figure 7. SolidWorks model of the control volume.

### Missile Design and Drawing:



### Missile model drawing steps in solidworks:

1. The steps outlined here were used to create the missile model used in the simulations. Start SolidWorks and select “New” and create a new part. Check under “Options,” “Units” that the selected units are “IPS” (Inch Pound Second).
2. Change the view to “Front” and select “Sketch.”

3. Start by drawing the missile body. Draw a rectangle about the origin with the following dimensions as shown in Figure 47. This is to place the moment reference at the origin where CFX computes the Torque. This step is important. Calculating the Torque on the missile otherwise is complicated.

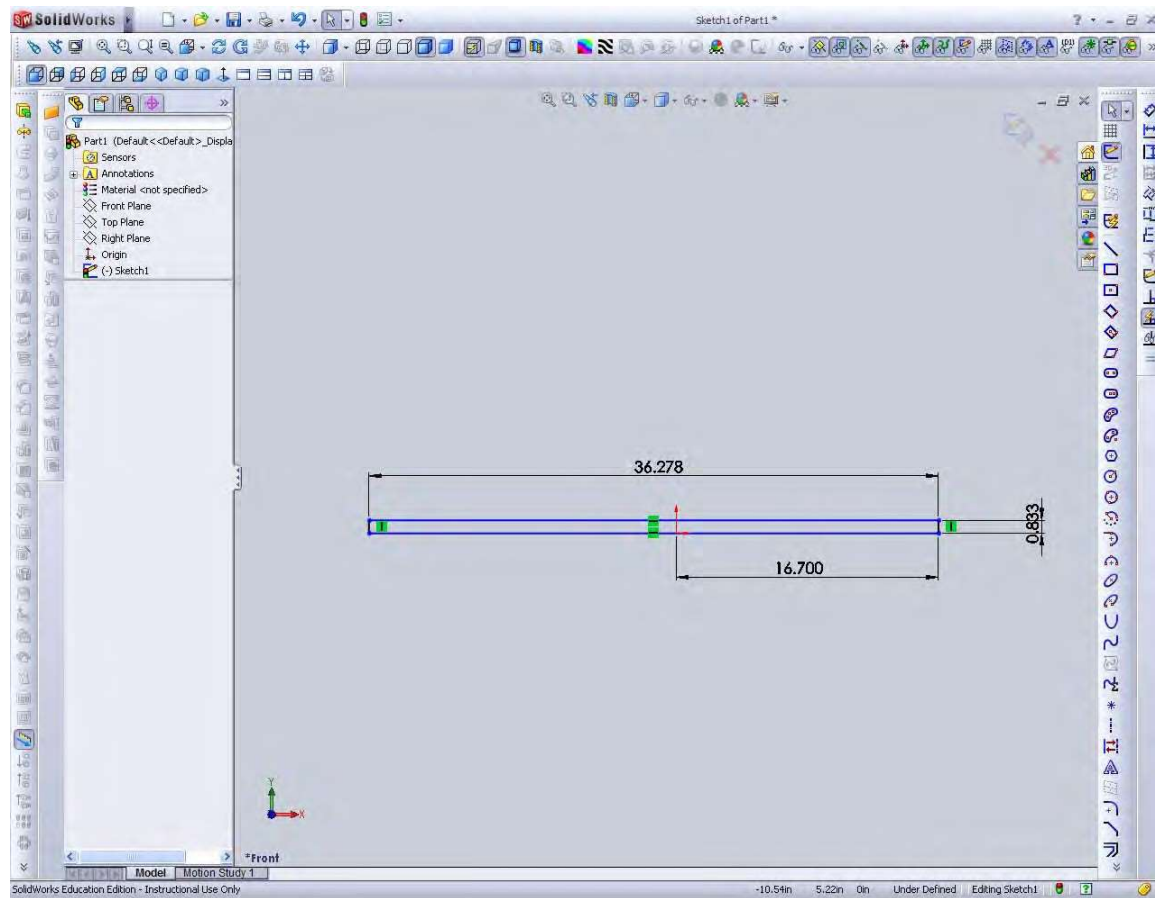


Figure 47. Placement of origin at missile moment reference.

4. Draw a “Center point arc” to form the hemispherical nose.

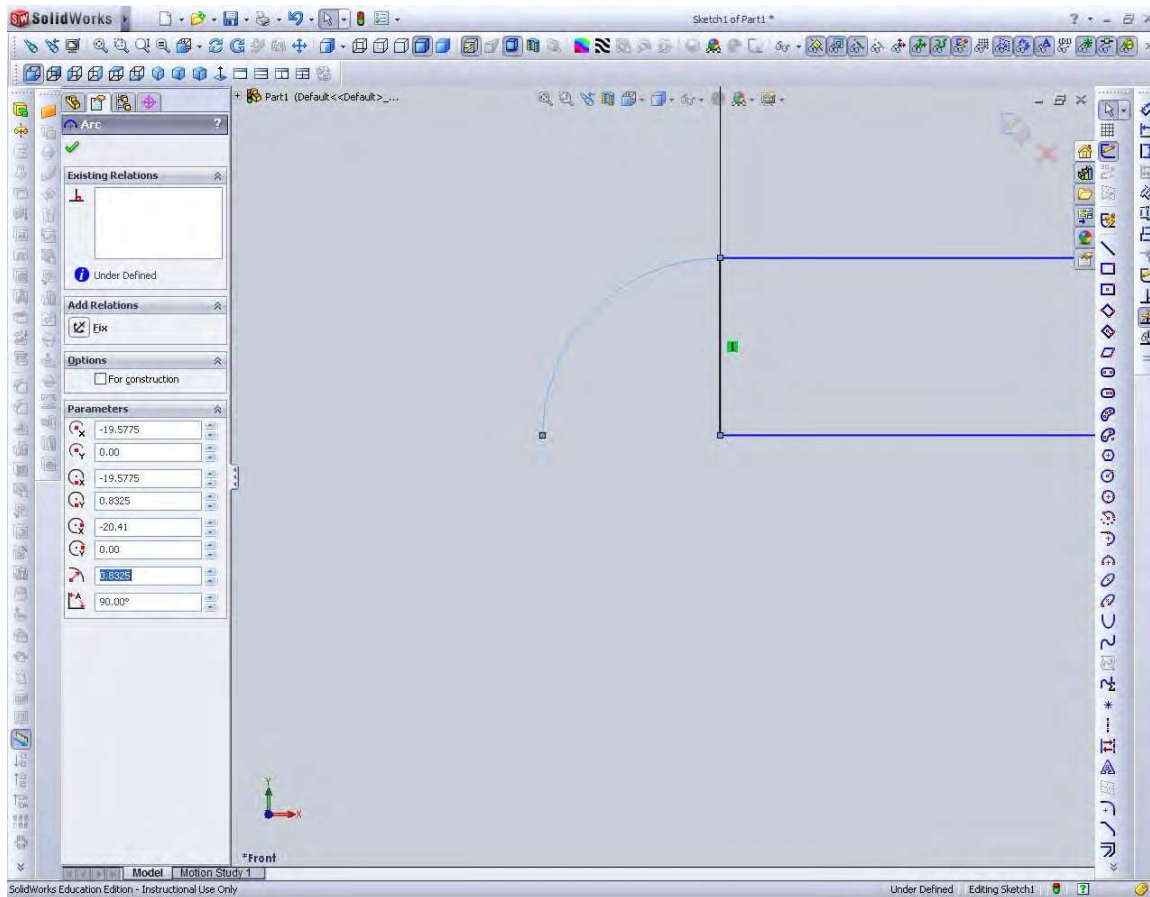


Figure 48. Drawing of hemispherical nose.

5. Draw line to close the body, and then delete the line separating the arc and rectangle to form a closed body.

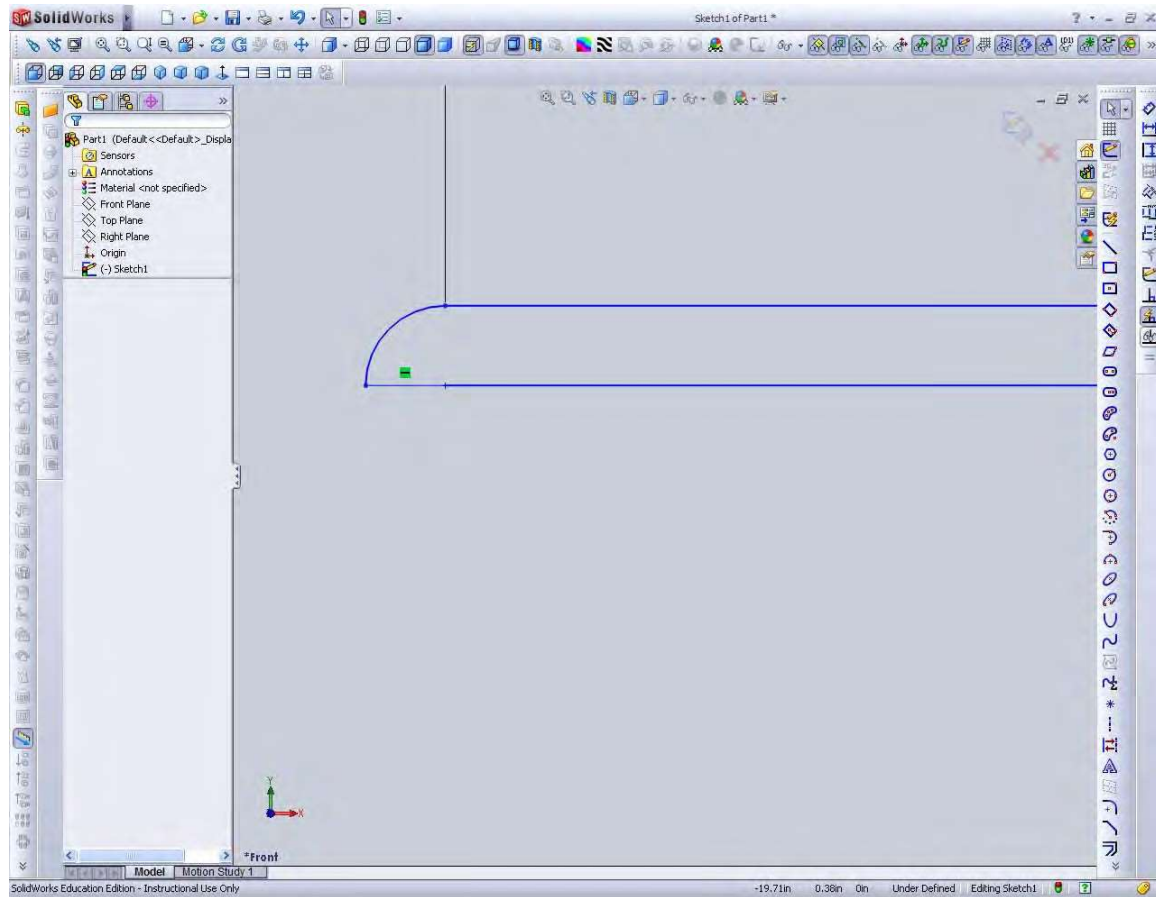


Figure 49. Completed cross section of missile body.

6. Select Revolved Boss/Base and then select center line. A cylinder should form. Click the green check to accept. Missile cylindrical body is now complete.

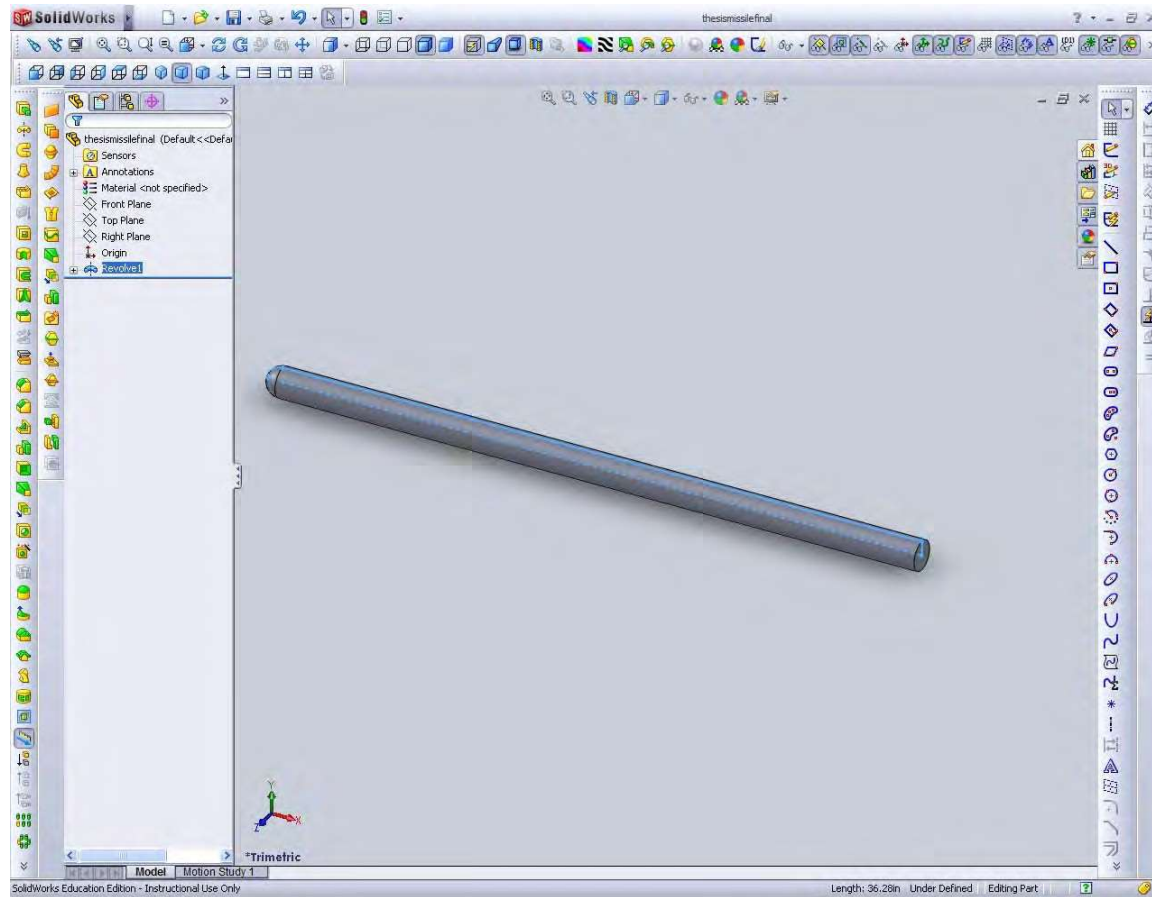


Figure 50. Completed missile body.

7. The hinge must be added to connect the canard to the missile body. Add construction lines and a point 5.3075 from the base of the nose cone. This is the center of the canard and the hinge. At this point, draw a circle centered on the hinge line of radius 0.08", then click the "Fully define sketch" button.

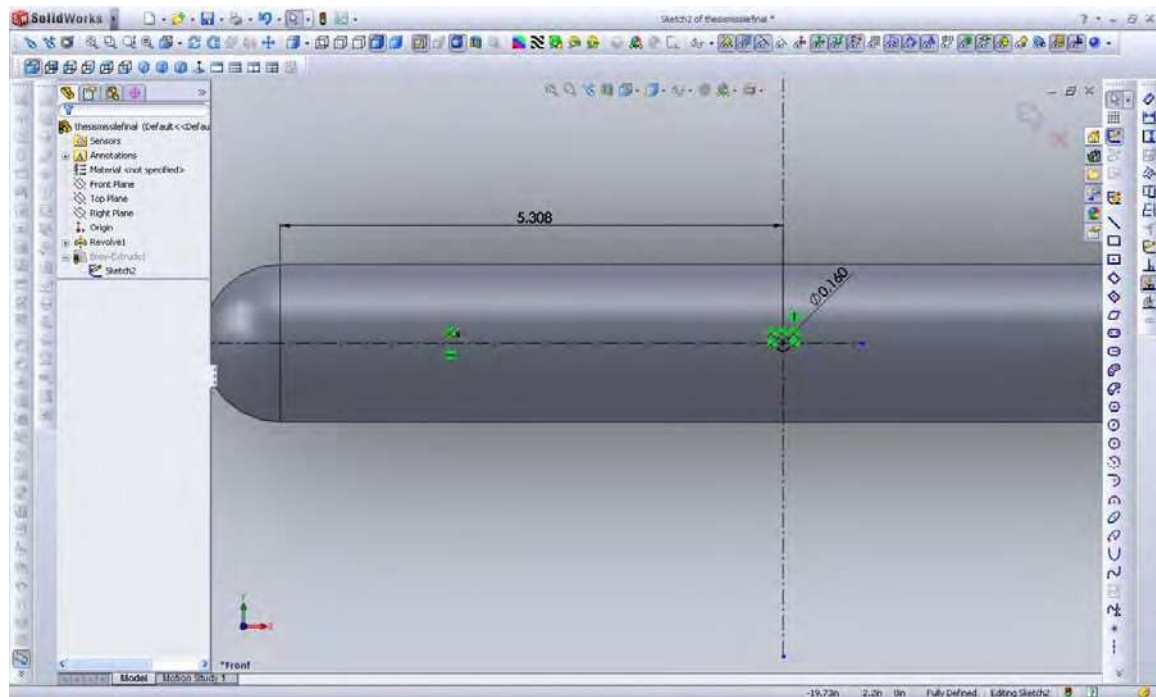


Figure 51. Sketching hinge of canard.

8. Extrude this circle by 0.8725" from the center. This will form the hinge of the canard.

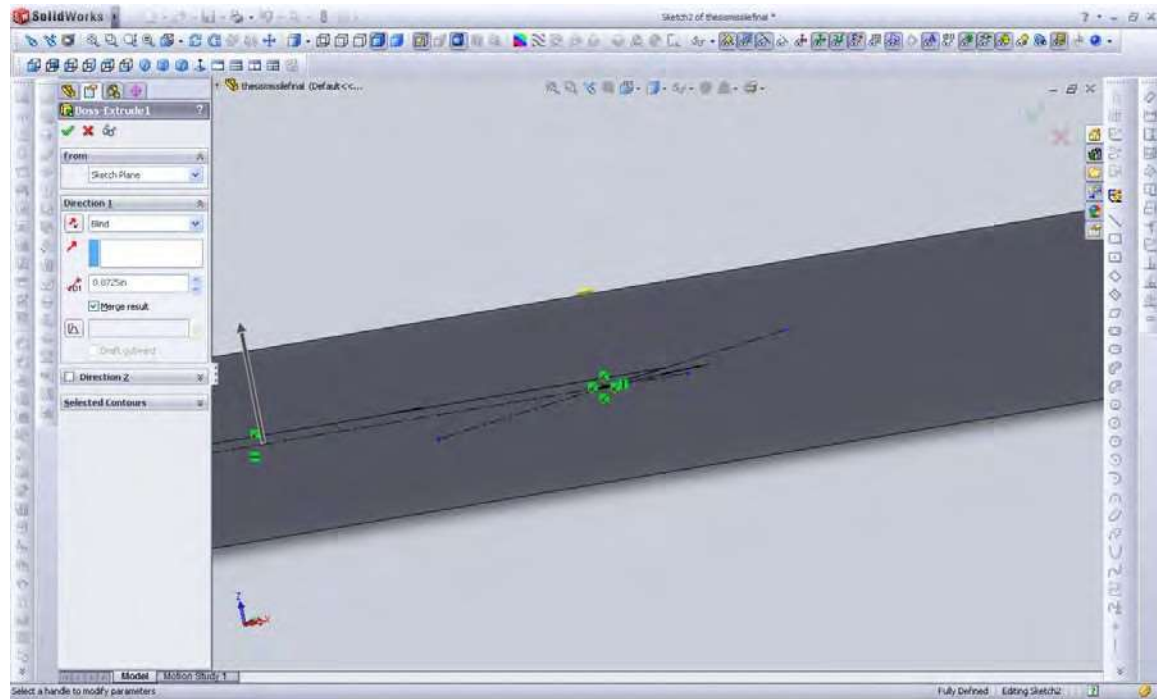


Figure 52. Extruding canard hinge from center of missile body.

9. Click “Insert – reference geometry – plane.” Select Front Plane as First Reference plane.

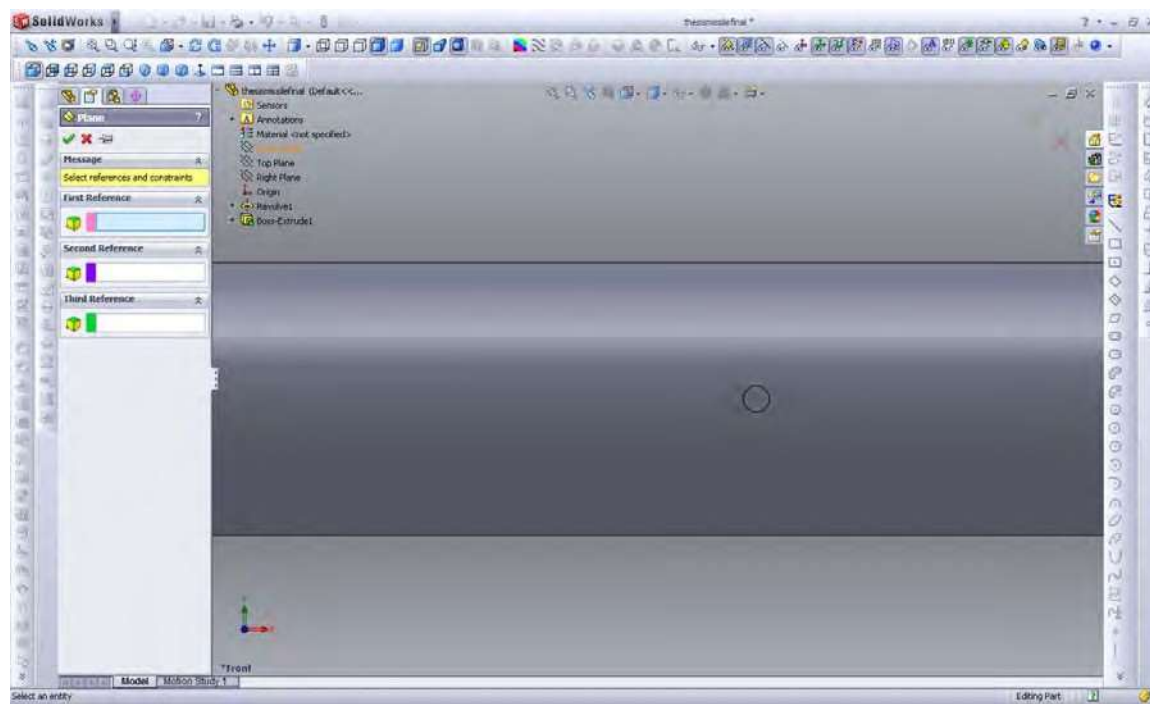


Figure 53. Add reference geometry window.

10. Set plane offset to 0.8725." This puts the plane at the tip of the hinge.  
Rename this plane "Canard Root Plane."

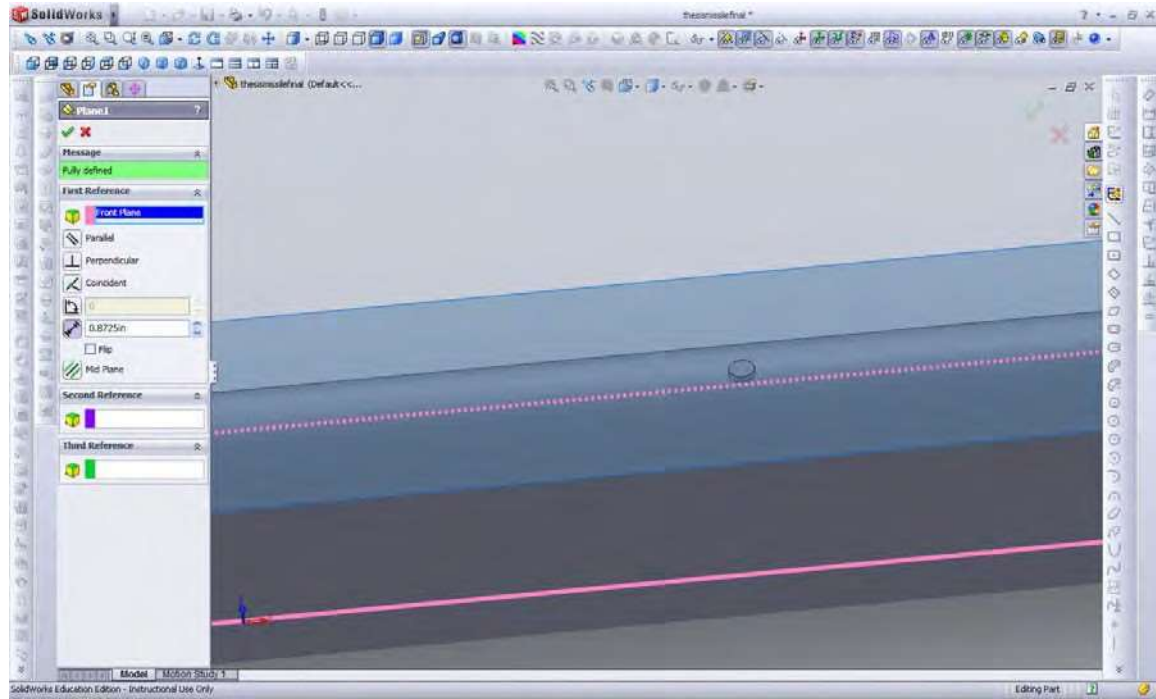


Figure 54. Adding reference plane at hinge tip.

11. Sketch a new drawing on the “Canard Root Plane.” Add a point at the center of the hinge and constructions lines.

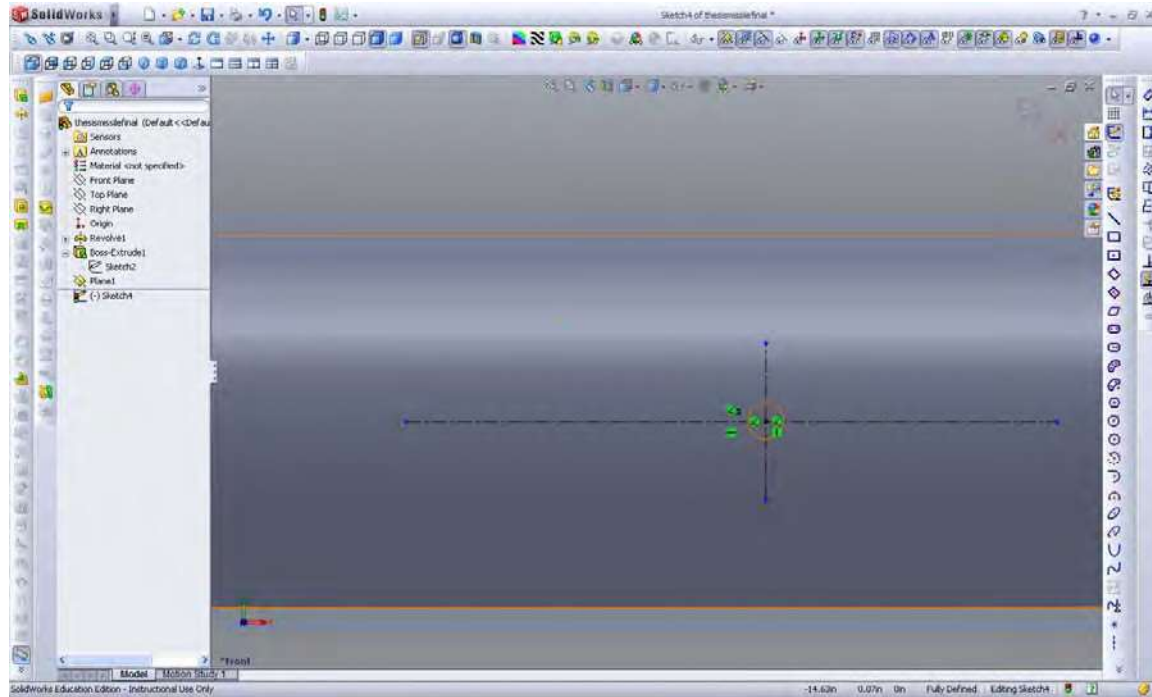


Figure 55. Adding construction lines for canard root.

12. Add 2 more points on the vertical construction line and dimension them to be 0.049" from the centre line.

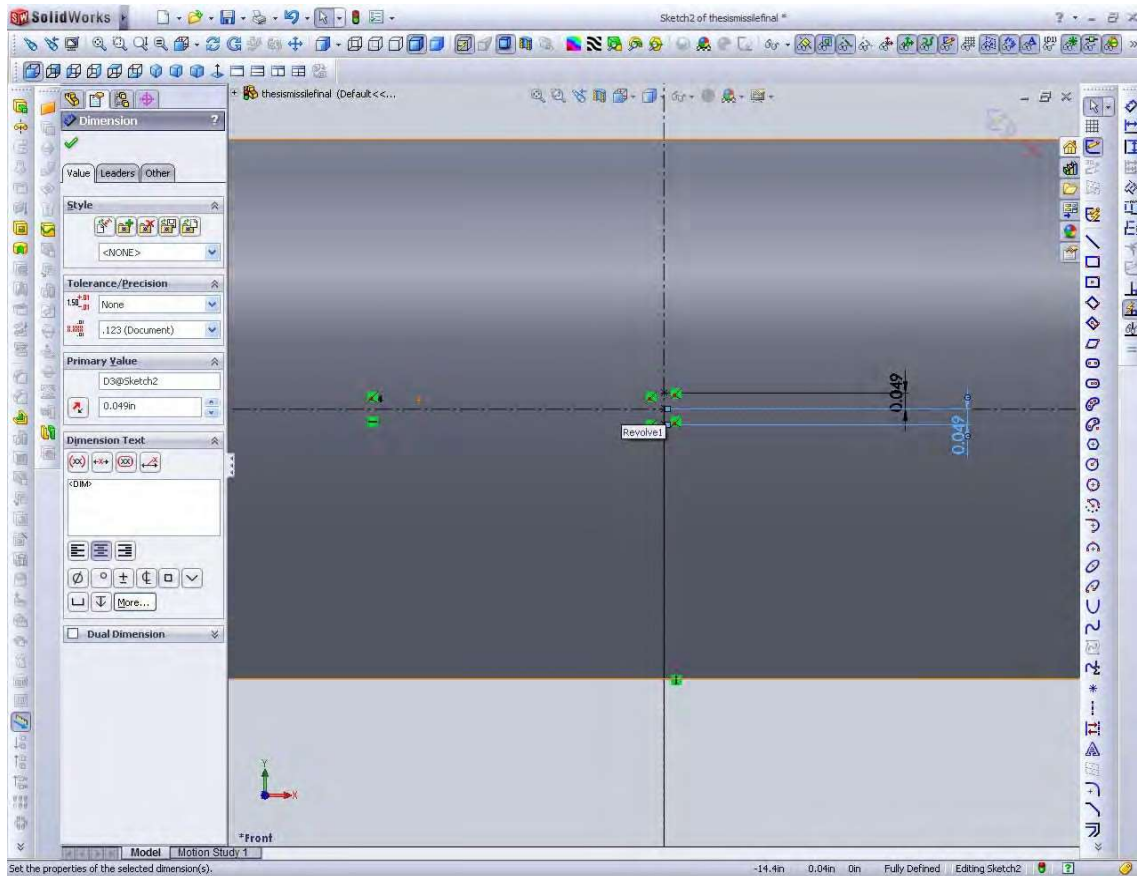


Figure 56. Adding canard thickness construction points.

13. Add another 2 points on the horizontal line and dimension them to form the leading and trailing edge of the root chord.

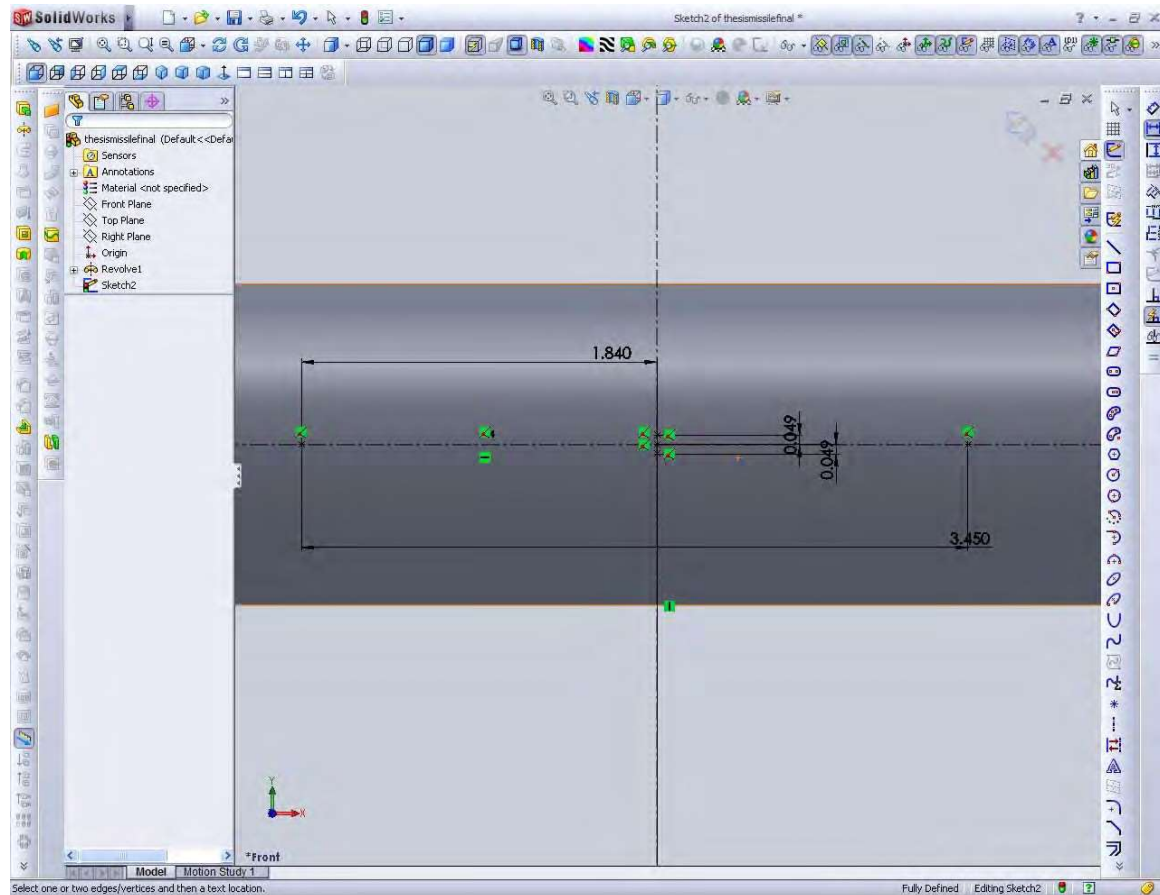


Figure 57. Adding leading and trailing edge construction points for canard.

14. Draw 2 lines to form the front wedge.

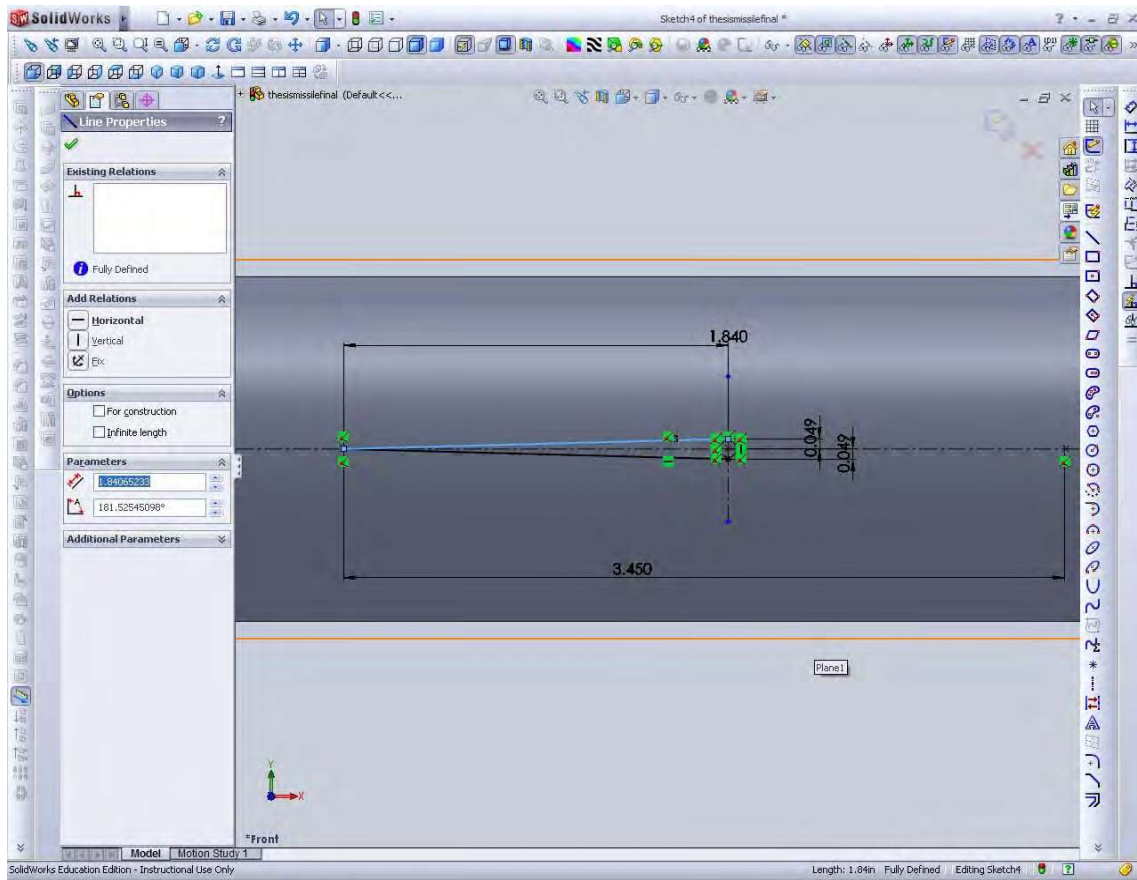


Figure 58. Drawing canard front wedge.

15. Add 2 more lines to create the trailing wedge. The sketch for the canard root is now complete.

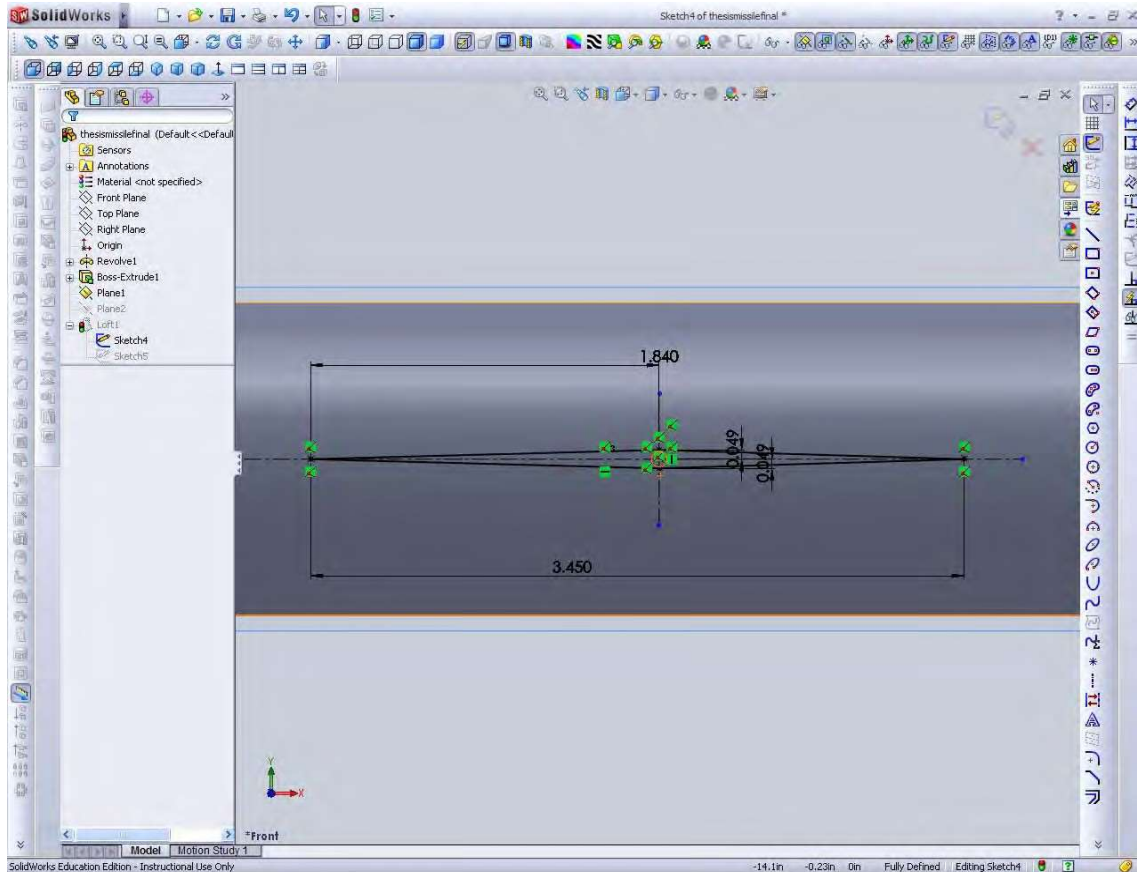


Figure 59. Drawing the trailing wedge of the canard.

16. Insert a 2<sup>nd</sup> reference plane “Canard Root Plane” as reference. The offset is the height of the canard. i.e. 1.72”. Rename this plane “Canard Tip Plane.”

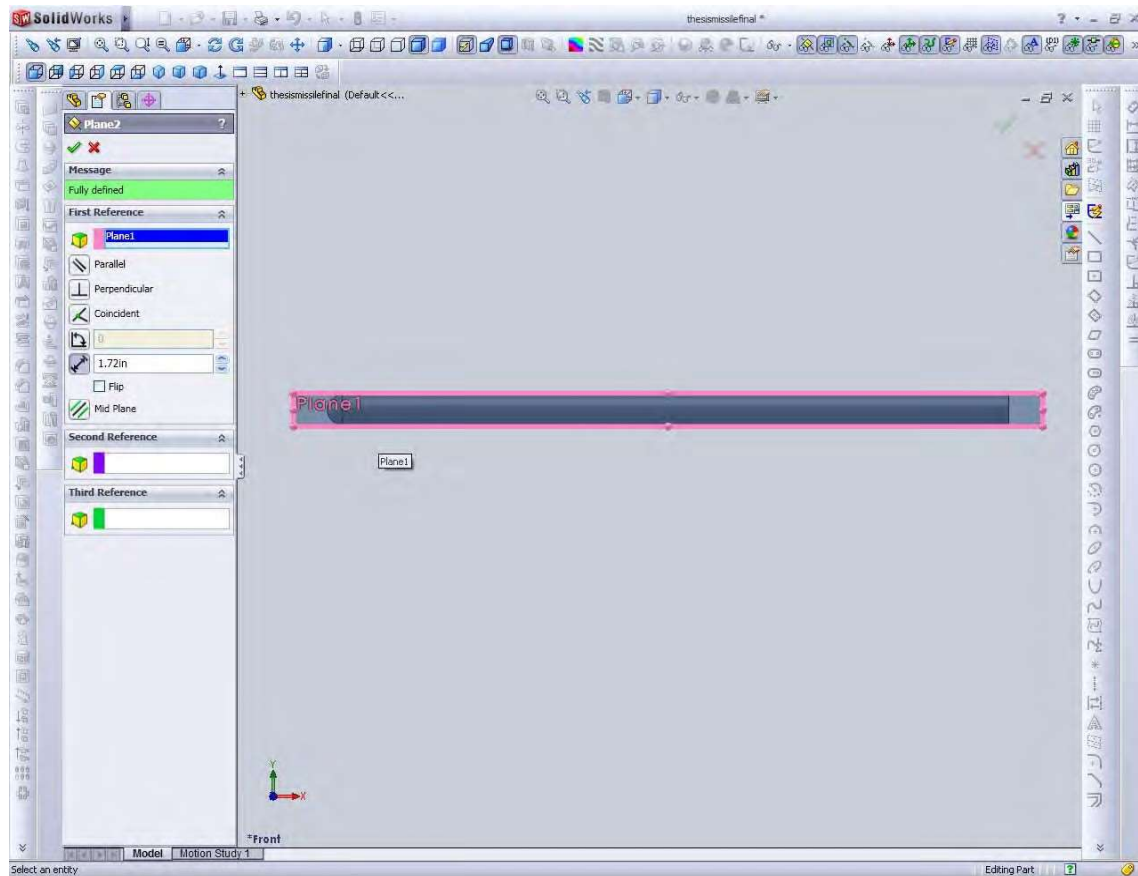


Figure 6o. Adding Canard Tip Plane.

17. Edit Sketch in “Canard Tip Plane.” Add a point and dimension it to the front tip of the canard as shown.

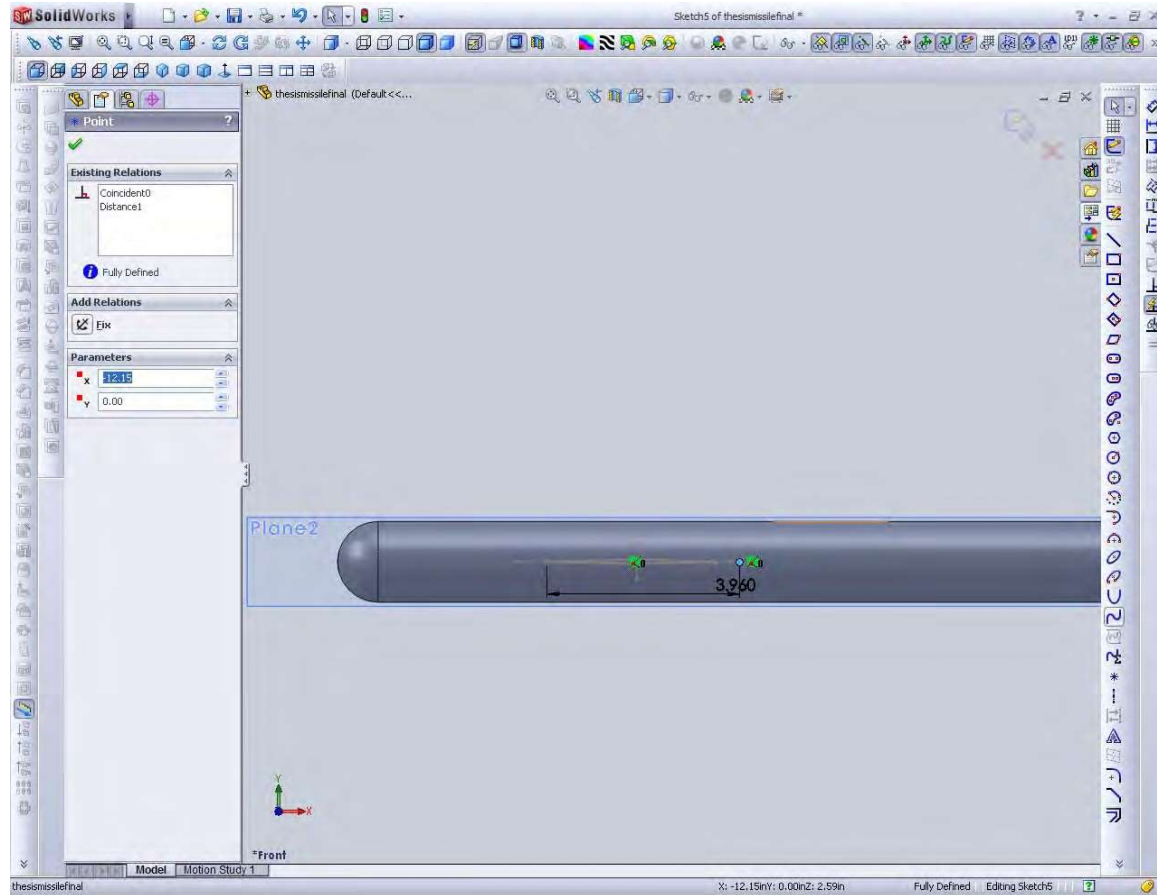


Figure 61. Adding canard tip.

18. Select Loft. Select the canard base and tip and add them to profiles.
- Preview the canard generated. Merge result should be checked.

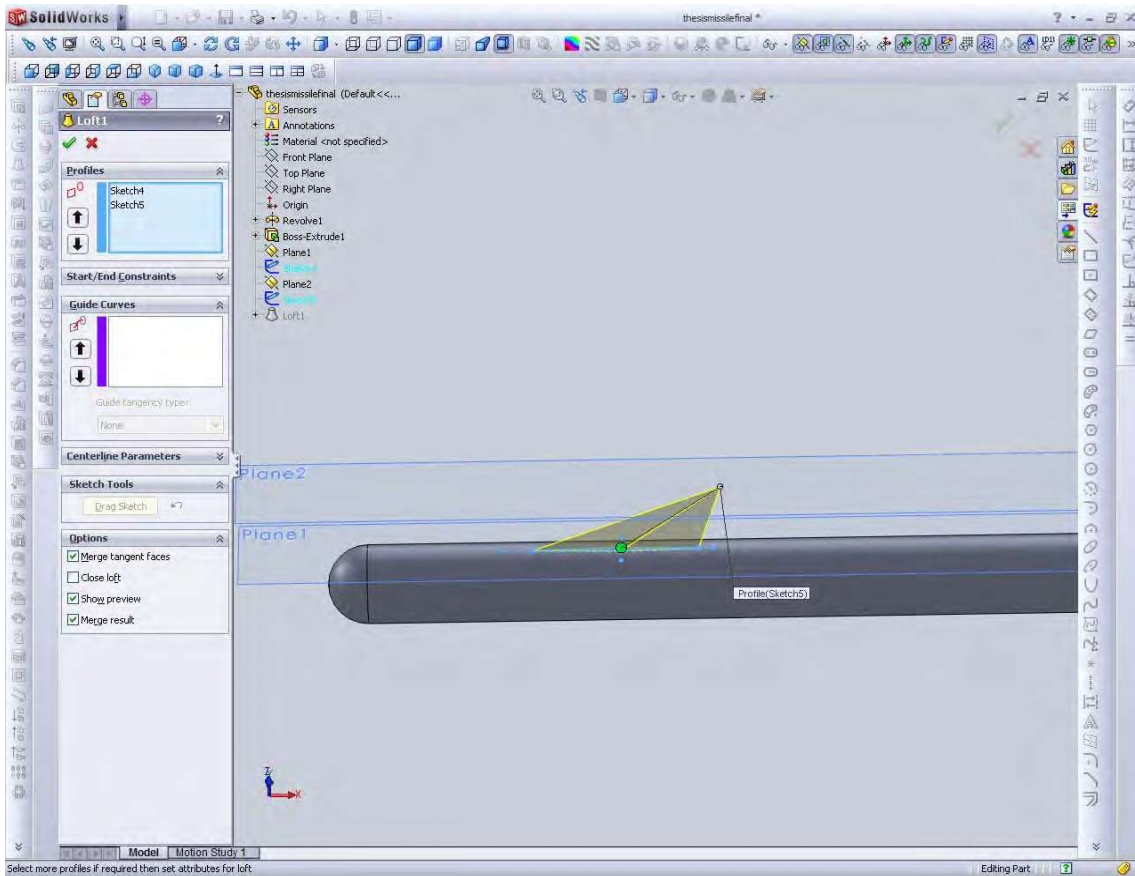


Figure 62. Loft to create canard.

19. Insert a 3<sup>rd</sup> reference plane using “Front Plane” as reference. The offset is the radius of the body 0.8325”. Rename this plane “Tail Root Plane.”

20. Edit Sketch on “Tail Root Plane.” Add construction lines and draw the general shape of the tail root. Dimension the root as shown.

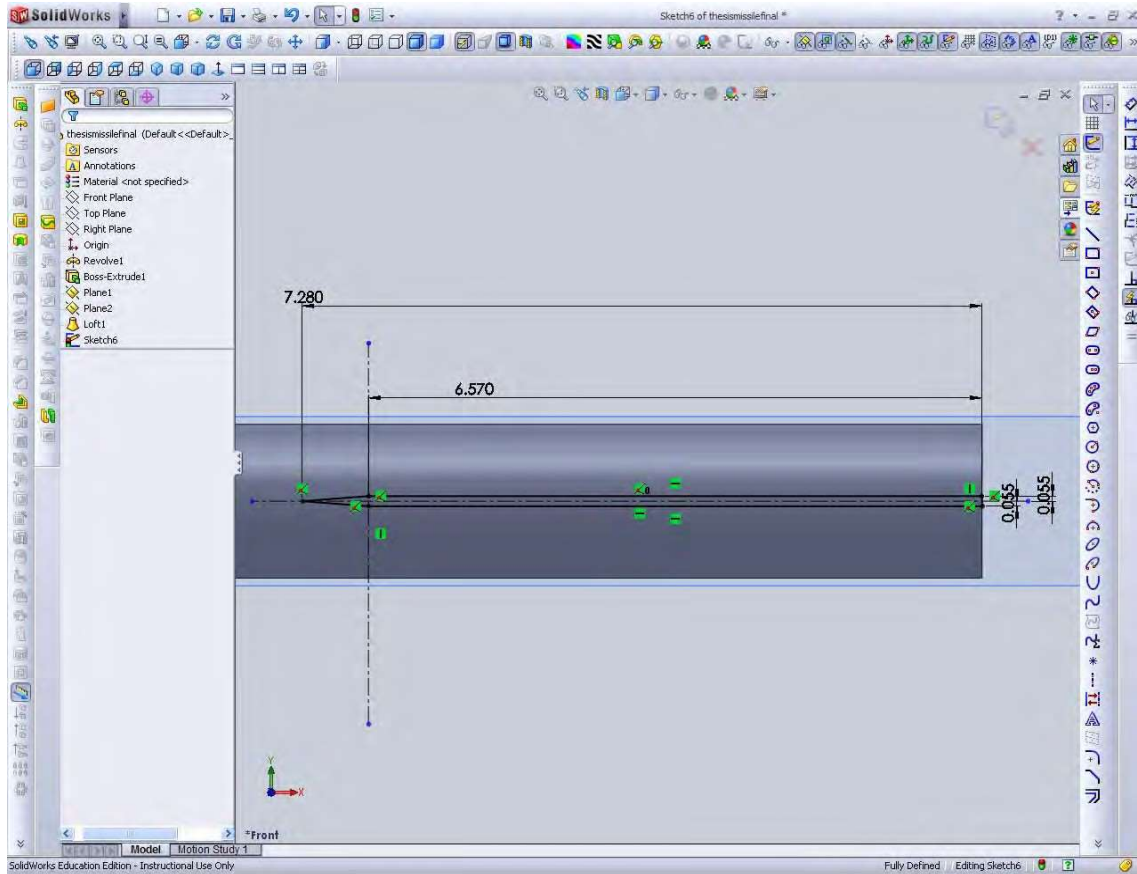


Figure 63. Adding Tail root.

21. Insert a 4<sup>th</sup> reference plane with “Tail Root Plane” as reference. The offset is the height of the wing. i.e. 2.54”. Rename this plane “Tail Tip Plane.”

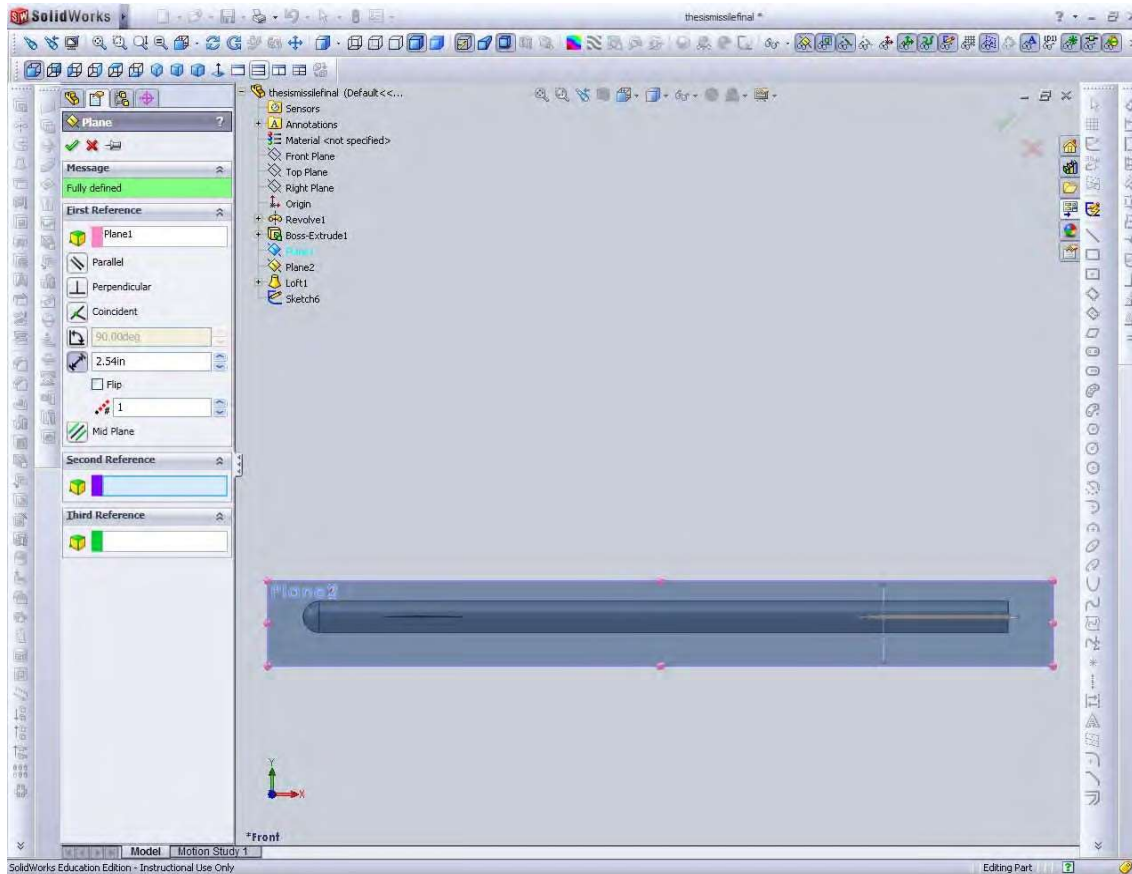


Figure 64. Adding Tail Tip reference plane.

22. Edit Sketch in “Tail Tip Plane.” Using the tail root as a reference for the sketch, draw the general shape of wing tip and dimension as shown.

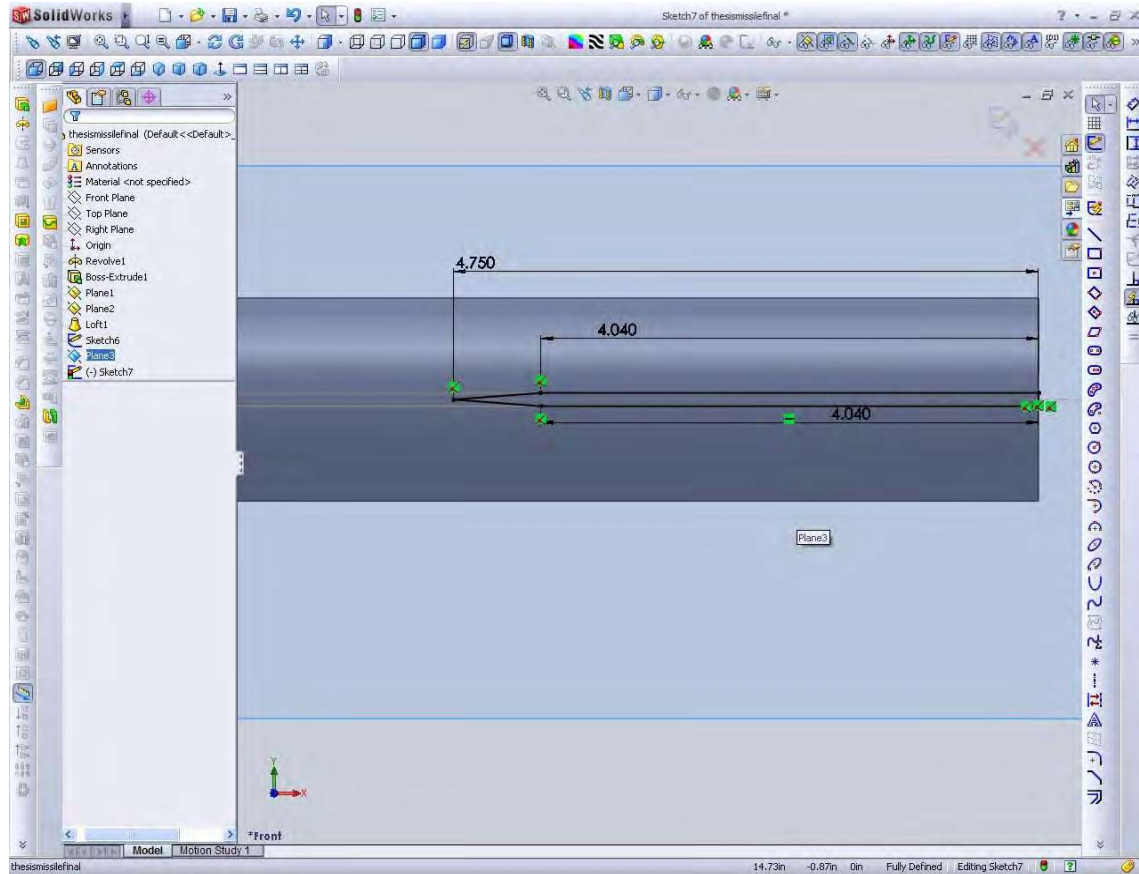


Figure 65. Adding Tail Tip on Tail Tip Plane.

23. Select Loft. Select the wing root and tip and add them to profiles. Preview the wing generated. If necessary, shift the loft start and end points to ensure the wing is lofted correctly. Merge result should be checked.

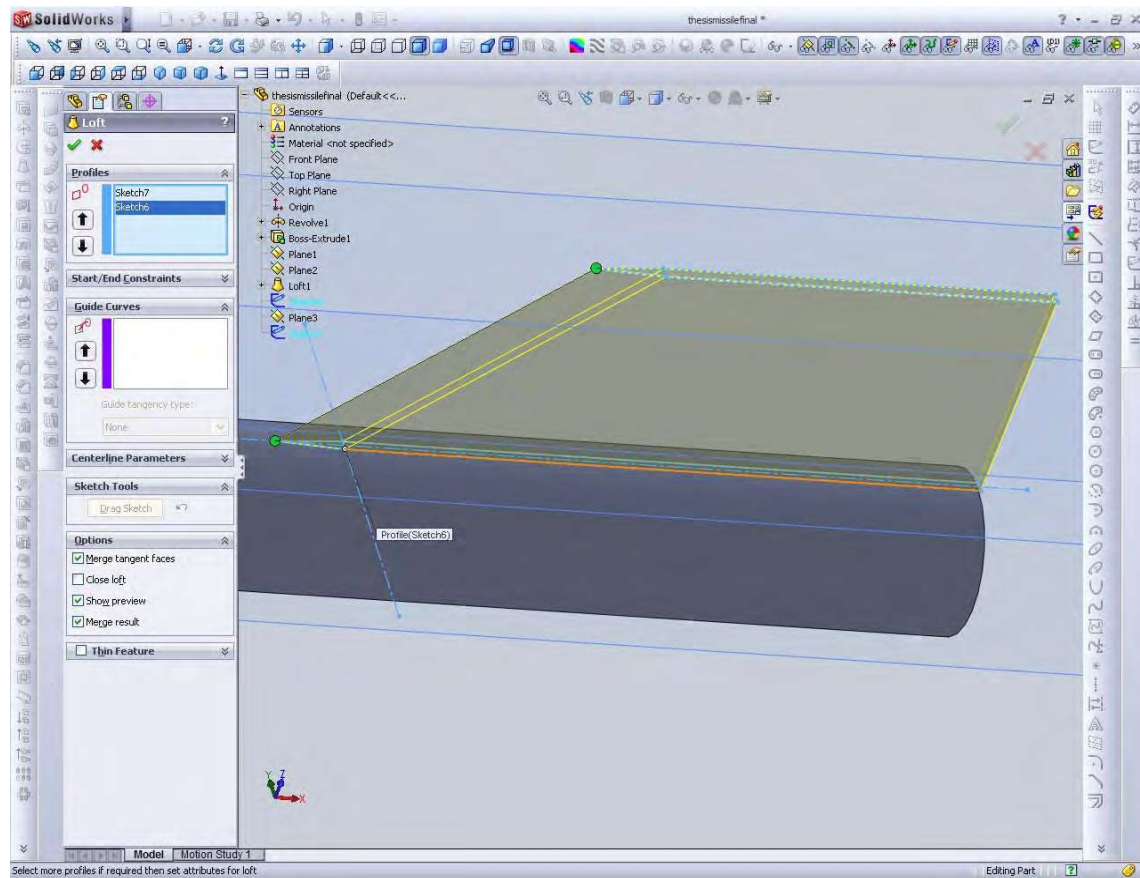


Figure 66. Loft to create tail.

24. Click “Extrude” and extrude the root of the wing into the body. Merge result should be checked. This mates the wing into the missile body.

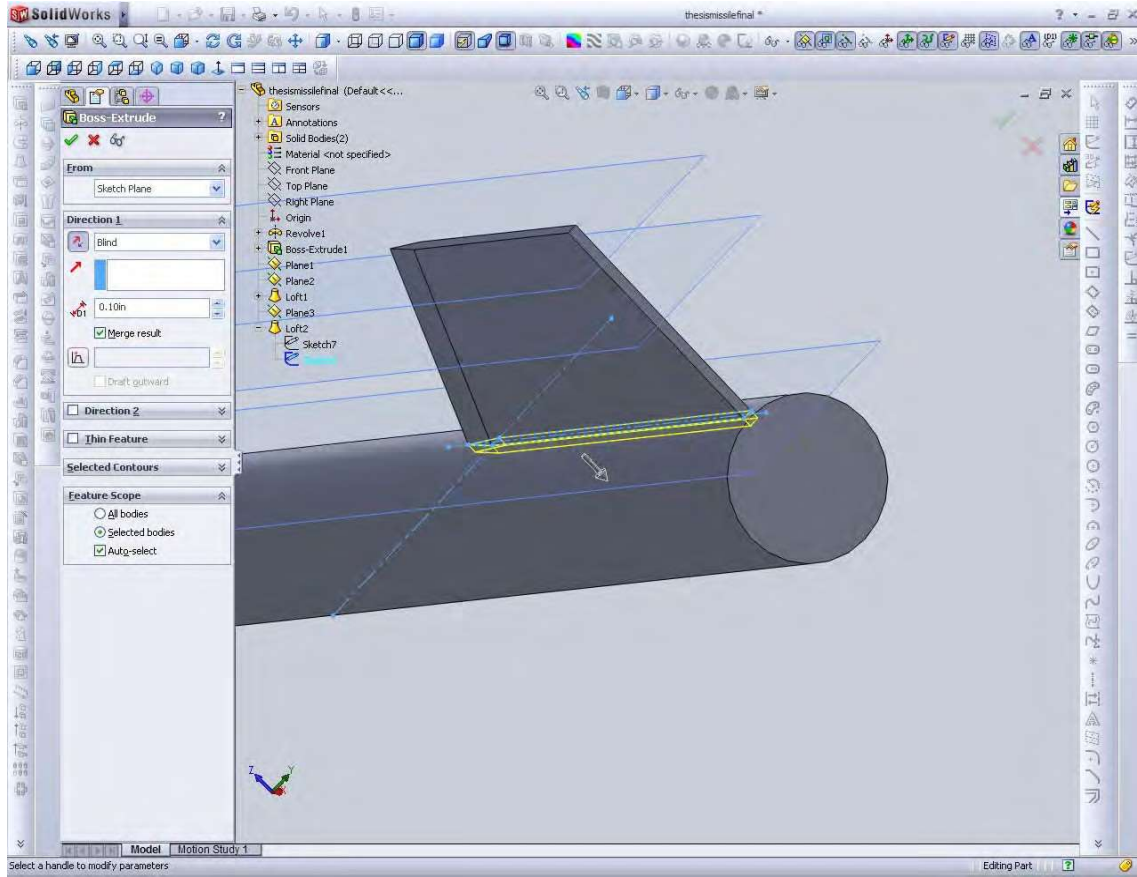


Figure 67. Mating Tail to missile body.

25. Select, Insert, Pattern/Mirror, Circular pattern. Under features to pattern, select the tail root extrusion first. Select the missile body as the axis for the pattern. Next add another circular pattern. This time select the loft. 3 additional tail fins should now be produced.

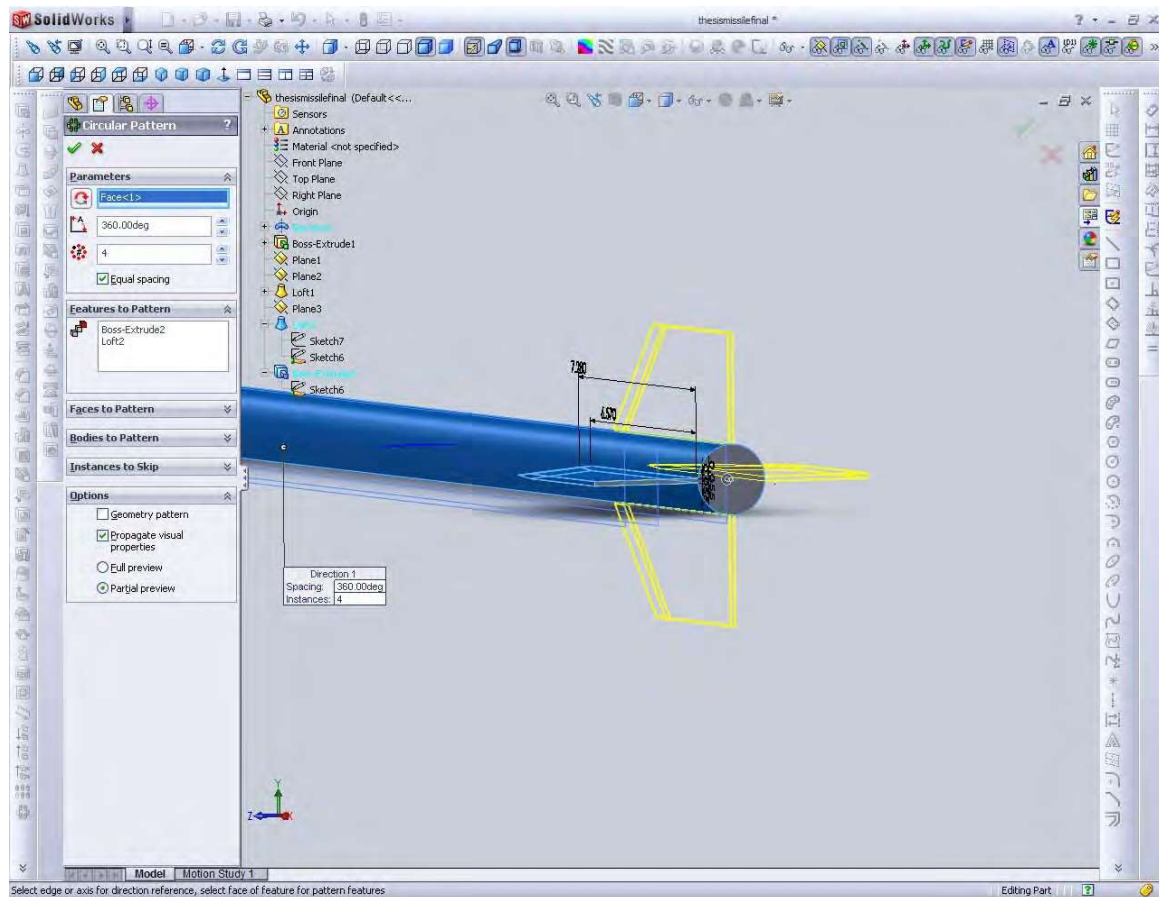


Figure 68. Patterning of tail fins.

26. Repeat for canard, starting with the hinge first. Select, Insert, Pattern/Mirror, Circular pattern. Under features to pattern, select the hinge extrusion first. Select the missile body as the axis for the pattern. Next add another circular pattern. This time select the canard loft. 3 additional canards should be produced. The missile is now complete.

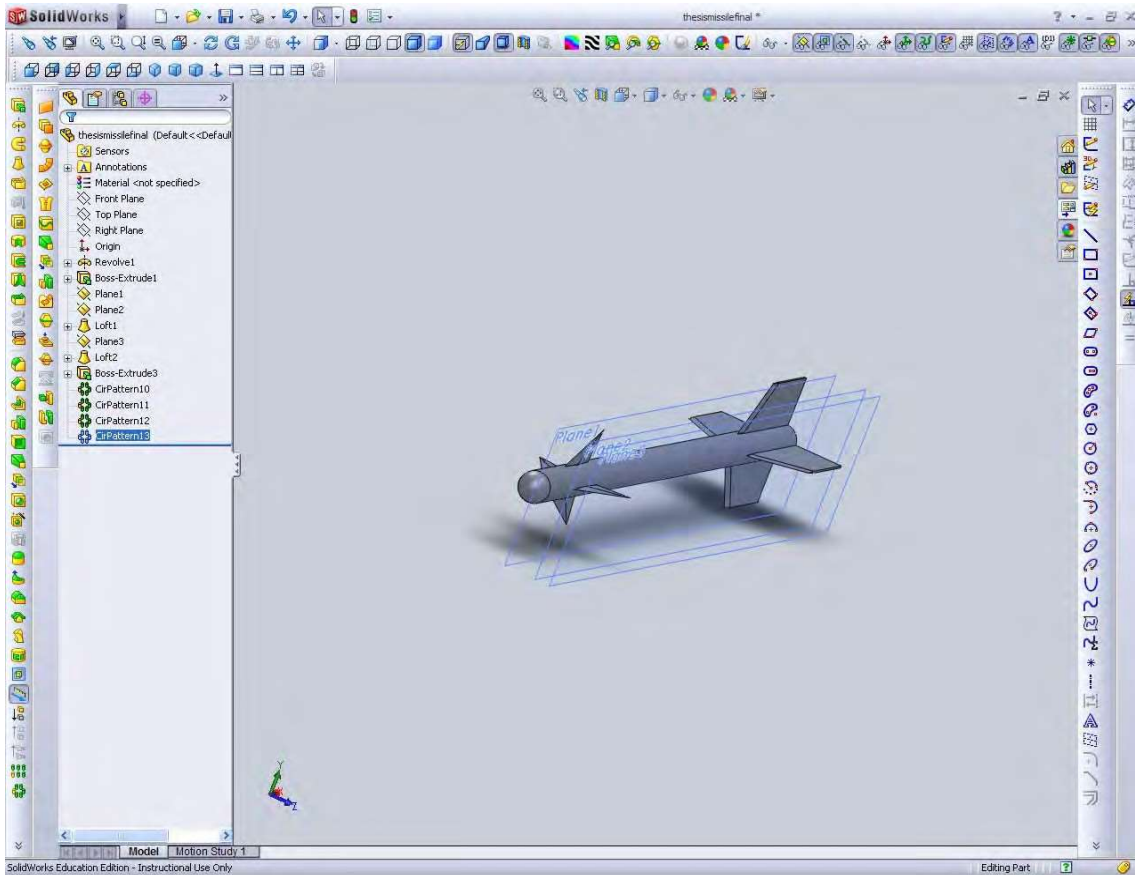


Figure 69. Completed missile model.

## A. IMPORT OF MODELS INTO DESIGNMODELER

ANSYS Workbench is first started and the CFX module is dragged into the main workspace, as shown in Figure 8.

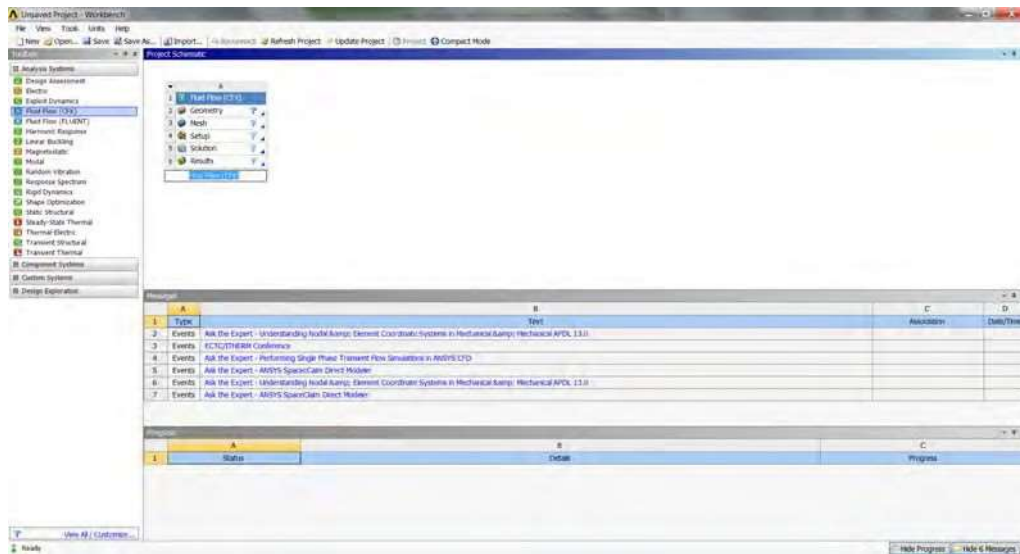


Figure 8. ANSYS Workbench GUI showing CFX in workspace.

DesignModeler is then started by double clicking on the “Geometry” tab in the CFX workspace. After DesignModeler loads, click “File” and select “Import External Geometry File.....”

In the pop-up dialog, select the parasolid file of the control volume and click “Open.” This will return you to DesignModeler. Check in the “Details view” that the “Operation” selected is “Add material.” Click “Generate” to generate the control volume in DesignModeler. Add the missile model now by repeating the same steps for importing external geometry. Prior to generating the model, the “Operation” option in the “Details view” should be changed to “Cut material.” After clicking “Generate,” DesignModeler should

cut out the volume of the missile model from the control volume. This is illustrated in Figure 9. This completes the import of the two parts into CFX.

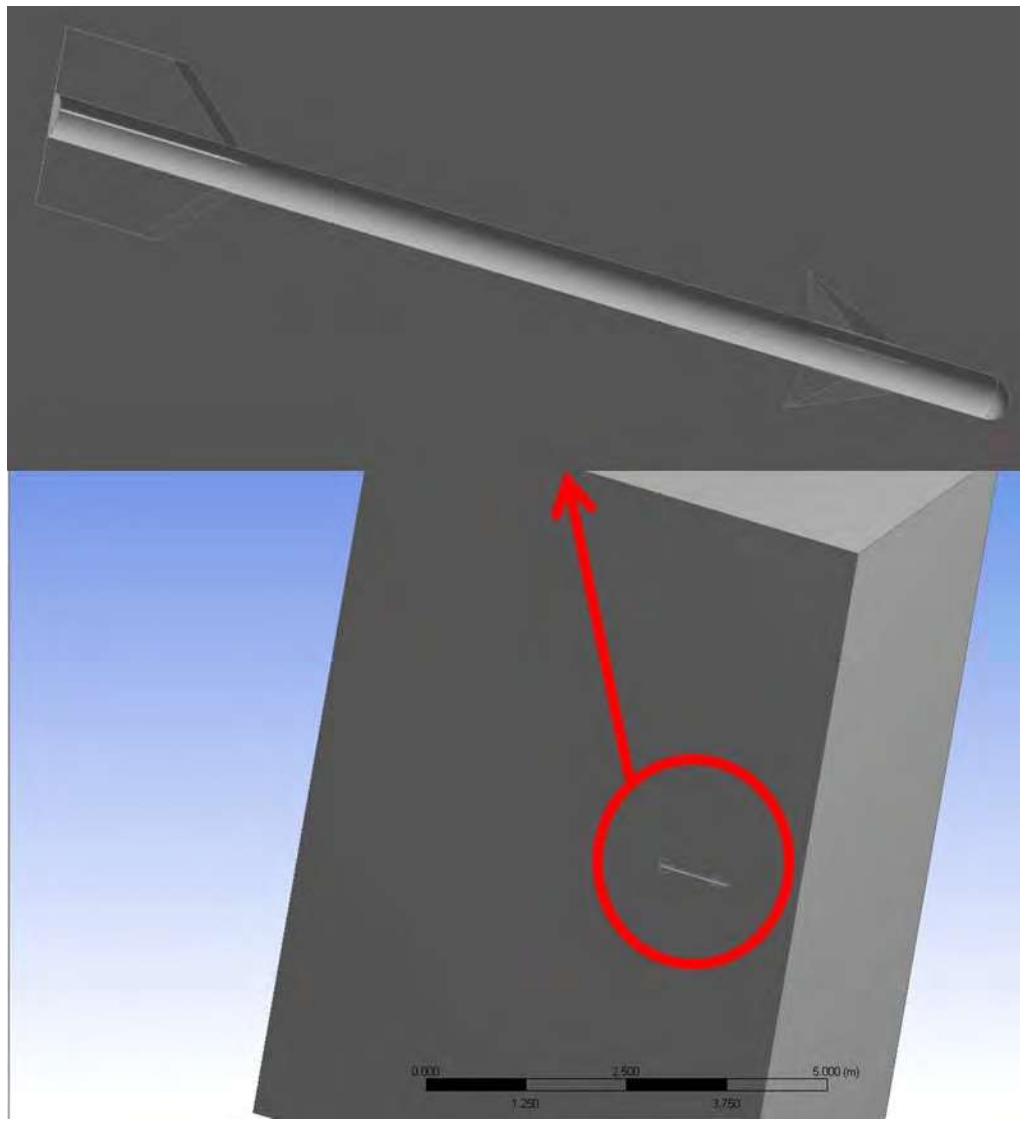


Figure 9. Control volume and missile model cutout.

## 1. MESHING

Meshering is started by double clicking on the “Mesh” tab in the CFX workspace. In Meshing, the six faces of the control volume have to be individually selected and named. This naming is used later in the Setup to identify the purpose of each of the six faces. Faces or geometries on the missile body can also be selectively named in order to perform additional refinement on these geometries. In this analysis, the canard leading and trailing edges as well as the leading edges on the tail were selected for additional refinement. The refinement setting used is summarized in Table 1.

Geometry	Refined part	Method	Number of Divisions
Canard 1 and 3 (Half body)	Leading and trailing edge	Edge	125
Canard 2 (Full body)	Leading and trailing edge	Edge	400
Tail 1 and 3 (Half body)	Leading edge	Edge	125
Tail 2 (Full body)	Leading edge	Edge	125

Table 1. Refinement settings.

## 2. COMMON MESH SETTINGS

The common mesh settings used for all the test cases are summarized in Table 2.

<b>Defaults</b>	
Physics Preference	CFD
Solver Preference	CFX
<b>Sizing</b>	
Use Advanced Size Function	On: Proximity and Curvature
Relevance Centre	Fine
Initial Size Seed	Active Assembly
Smoothing	Medium
Transition	Slow
Span Angle Centre	Fine
Curvature Normal Angle	10°
Proximity Accuracy	0.5
Num Cells Across Gap	Default (3)
Min Size	1.e-004 m
Max Face Size	5.e-002 m
Max Size	0.5 m
Growth Rate	Default (1.2)
Minimum Edge Length	4.5361e-005 m

Table 2. Common mesh settings.

### 3. INFLATION SETTINGS

The entire missile body was also selected and named to facilitate the addition of an inflation layer on the entire missile body. The Table 3 summarizes the inflation settings used for the missile model for each case.

Inflation	Case 1 M=0.2	Case 2 M=0.8	Case 3 M=1.2
Inflation Option	Total Thickness	Total Thickness	Total Thickness
Number of Layers	10	20	20
Growth Rate	1.2	1.2	1.2
Maximum Thickness	1.e-003 m	3.e-003 m	3.e-003 m

Table 3. Inflation settings for each test case.

### 4. MESH QUALITY

In general, a good quality mesh can be defined as one that has the proper refinements around the primary areas of interest. The edges and shape of the geometry should also remain well defined and not altered by the mesh in any way. A proper inflation layer growing outward from the body is also necessary to produce better definition of the boundary layer. An all quad mesh is preferred for computational purpose and a sweep of the computational domain with quad elements was attempted but was disallowed by the mesher. Therefore a large number of triangular elements

had to be created instead in order to mesh the body and control volume. Figure 10 show the mesh for test case 1.

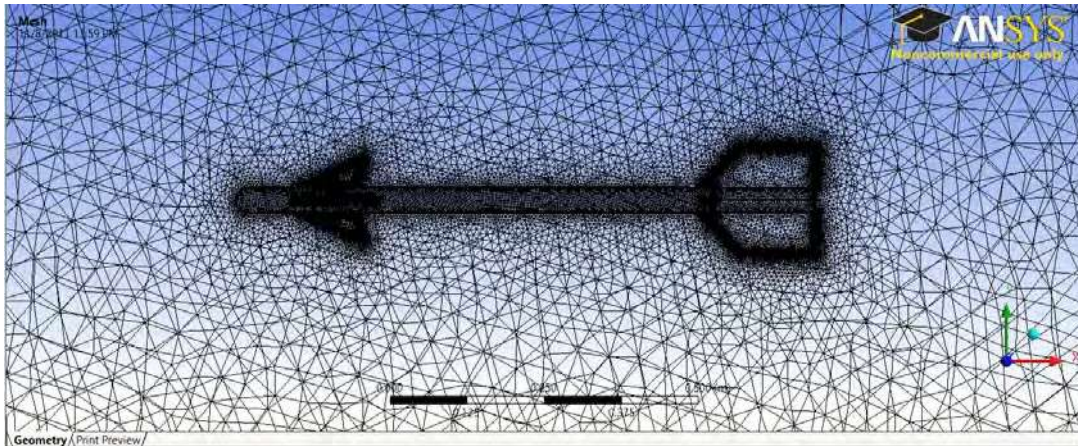


Figure 10. Mesh of missile model and control volume for test case 1.

## B. SETUP OF CFX-PRE (SETUP)

### 1. GENERAL SETUP

Setup is started by double clicking on the “Setup” tab in the CFX workspace. The method employed to simulate an AOA in the control volume is to have two inlets and two outlets. The inlets will have both a  $u$  and  $v$  velocity components which would be the product of the sine and cosine of the AOA and the test case Mach number (Figure 11). For the 0 AOA case, the upper and lower boundaries are openings rather than outlet and inlet, respectively.

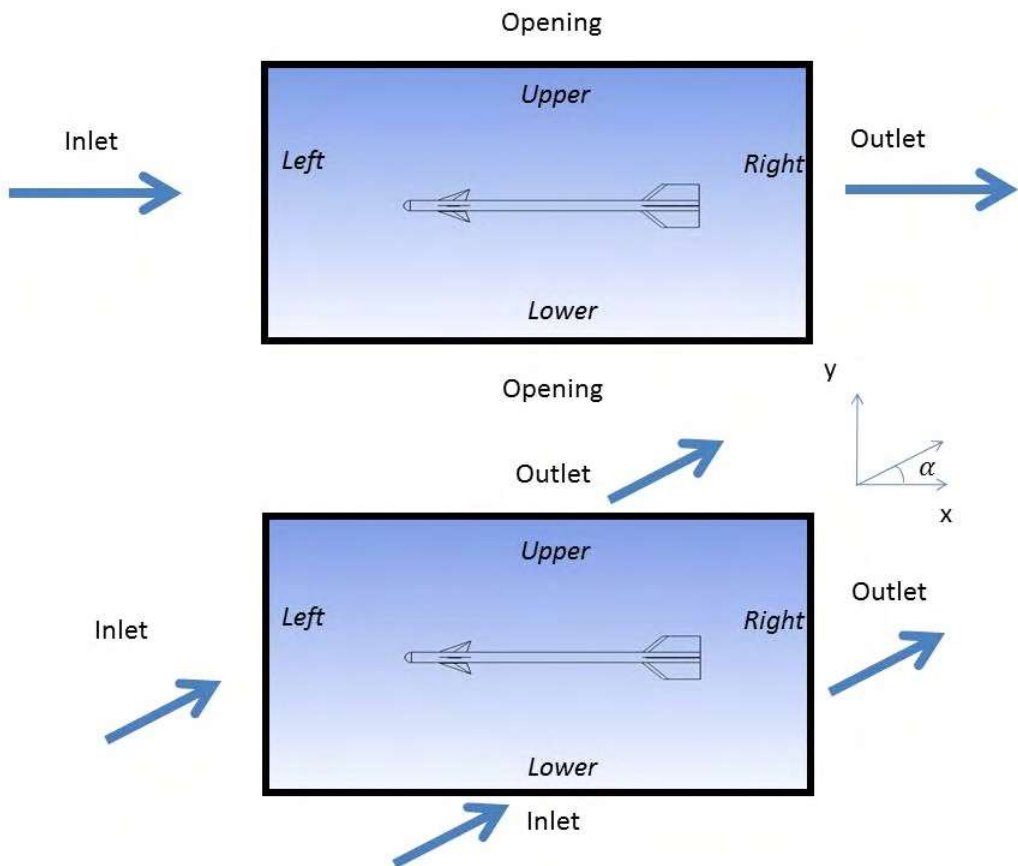


Figure 11. Setup of control volume for AOA.

This method is selected as it allows the reuse of the same mesh for all simulation runs at the same Mach number by just updating the inlet velocity components. An alternate approach is to tilt the entire missile body using DesignModeler to simulate an AOA (Figure 12). This approach however requires that each AOA case have a separate mesh and hence increases the computational time required to run all the test cases. The earlier approach is therefore selected for this analysis.

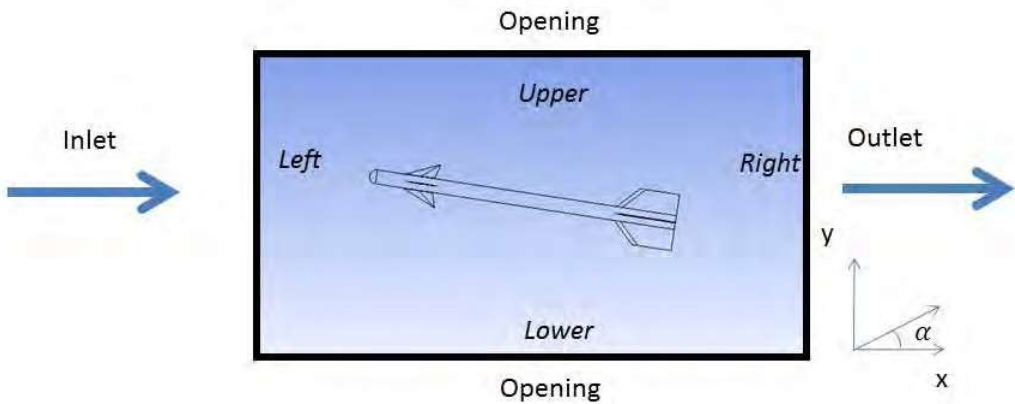


Figure 12. Alternative method for setup control volume for AOA.

## 2. ASSIGNMENT OF BOUNDARIES

Setup requires the assignment of boundaries to the Named Selections identified in Meshing. These boundaries are defined to be the Inlet, Outlet, Opening, Symmetry and Walls of the control volume. All undefined boundaries are Walls by default. Figure 11 shows the boundaries and their assignments. The front and back faces in the plane of the paper are assigned as Opening and Symmetry, respectively.

## 3. PARAMETERS SETUP

### a. Analysis Type and Material Setup

The default Analysis Type specified should be Steady State. This should be checked under “Simulation,” “Analysis Type” then “Analysis Type”

entry. Under the “Default Domain” tab, the Material selected should be Air Ideal Gas. The next tab should be marked “Fluid Model.” Under this tab, the heat transfer option selected was “Total Energy” and the Turbulence Model selected was “Shear Stress Transport.” The option for the “High Speed (compressible) Wall Heat Transfer Model” should also be checked.

### b. Inlet Setup

After all the boundaries have been added and named, each of the boundaries must be set up for the simulation to run. For inlet boundaries, the “Flow Regime,” “Mass and Momentum,” “Turbulence” and “Heat Transfer” need to be set. Figure 13 illustrates an example of the input for the Mach 0.2 case at 2 deg AOA.

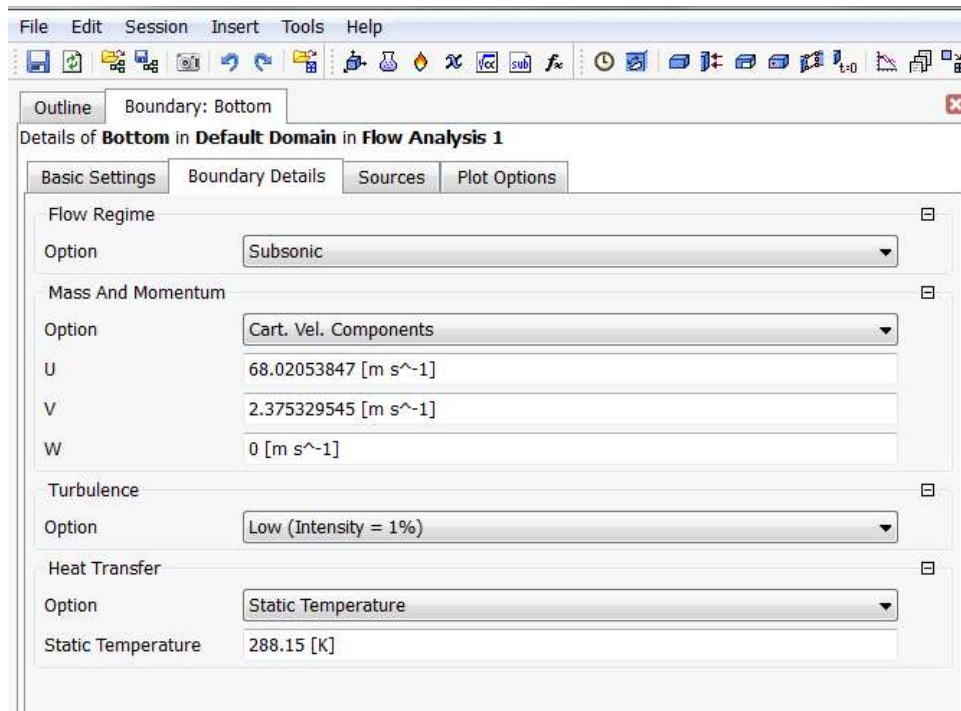


Figure 13. Boundary details for M=0.2 test case at 2 deg AOA.

### c. Outlet Setup

Outlets are configured with just “Flow Regime” and “Mass and Momentum” settings. Figure 14 illustrates an example of an Outlet configuration used.

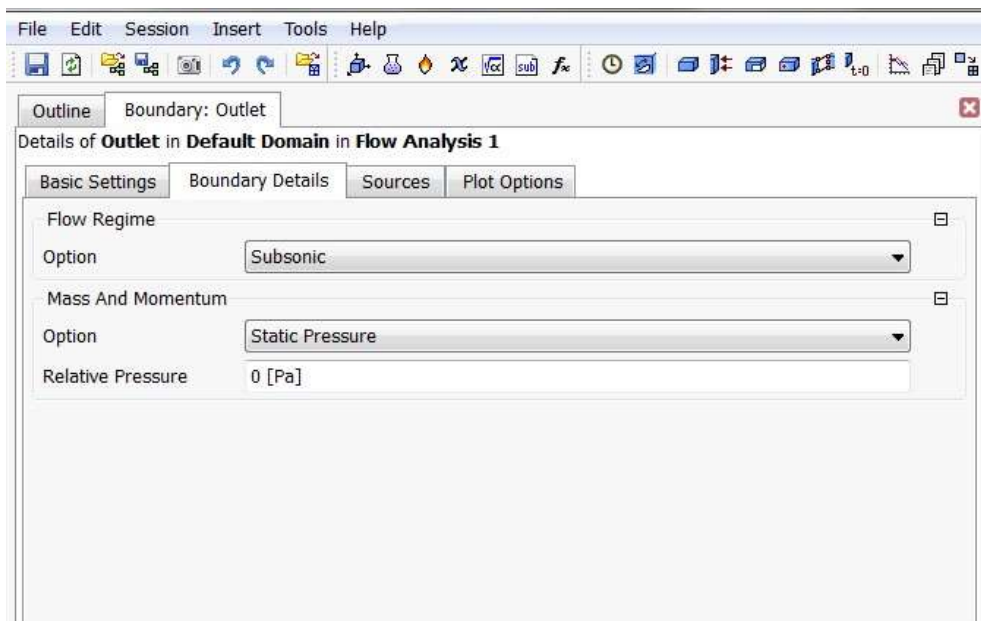


Figure 14. Outlet settings.

### d. Opening Setup

Openings differ from inlets and outlets as they allow inflow and outflow across the boundary whereas inlets and outlets only allow flow in one direction. Entrainment was also selected as this was recommended by the

program. Zero gradient turbulence option was also a recommendation as a result of using Entrainment in the Mass and Momentum option. Figure 15 illustrates an example of settings used for an Opening.

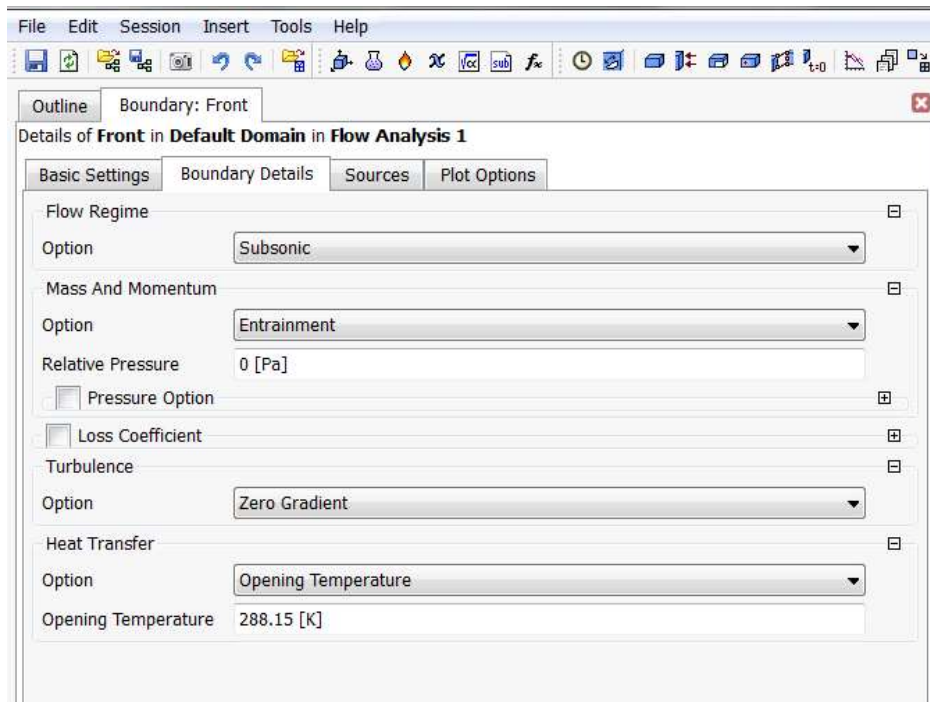


Figure 15.      Opening settings.

#### e.      Symmetry Setup

A symmetry boundary was identified and configured in the simulation.

This setting requires no additional setup besides identifying the boundary as symmetry.

#### f.      Solver Control Setup

In solver control, the “Max Iterations” was set to 100 and the “Residual Target” option was set to  $1 \times 10^{-6}$ . The “Advection” and “Turbulence” options were both set to “High Resolution.” Under the “Advanced Options” tab, all options under “Compressibility Controls” are checked.

#### **g. Expert Parameters**

“Expert Parameter” option was added to the simulation by selecting “Insert,” “Solver” then “Expert Parameter.” Under the convergence control tab, the “High Speed Models – max continuity loops” option was checked and assigned a value “3.”

## C. OBTAINING SOLUTIONS FROM CFX

### 1. STARTING THE CFX-SOLVER MANAGER

CFX-Solver Manager is started by double clicking on the “Solution” tab in the CFX workspace. The “Define Run” dialog is first displayed. This dialog allows partitioning of the problem as well as adjusting the memory allocation to each of the processing stages of the solver. For this simulation, the default memory settings were used.

### 2. PARTITIONING THE PROBLEM

In order to reduce computational time, the problem can be split up into several parts and solved in parallel. In this simulation, the problem was split up into eight parts to fully utilize the quad-Core processor in the computer used to run ANSYS. The “Run Mode” was selected to “HP MPI Local Parallel” and the number of partitions increased to eight.

### 3. DISPLAY MONITORS

The display monitors show the progress of the simulation in terms of the value of the residuals and plots the residuals. The display monitors also show all errors that may result from the simulation as well as the total time taken for the simulation to complete. A screenshot of the display monitors is shown in Figure 16. For these situations, the results may also not be as accurate as expected. As such, the mesh should be refined further and the simulation rerun. This is an iterative process that is very time consuming. In some cases, the residuals start to oscillate and further convergence is not possible. In such situations, the simulation can be stopped prematurely and the result at that iteration can be taken as the final result. A minimum convergence down to  $1 \times 10^{-4}$  is required for reasonable results.

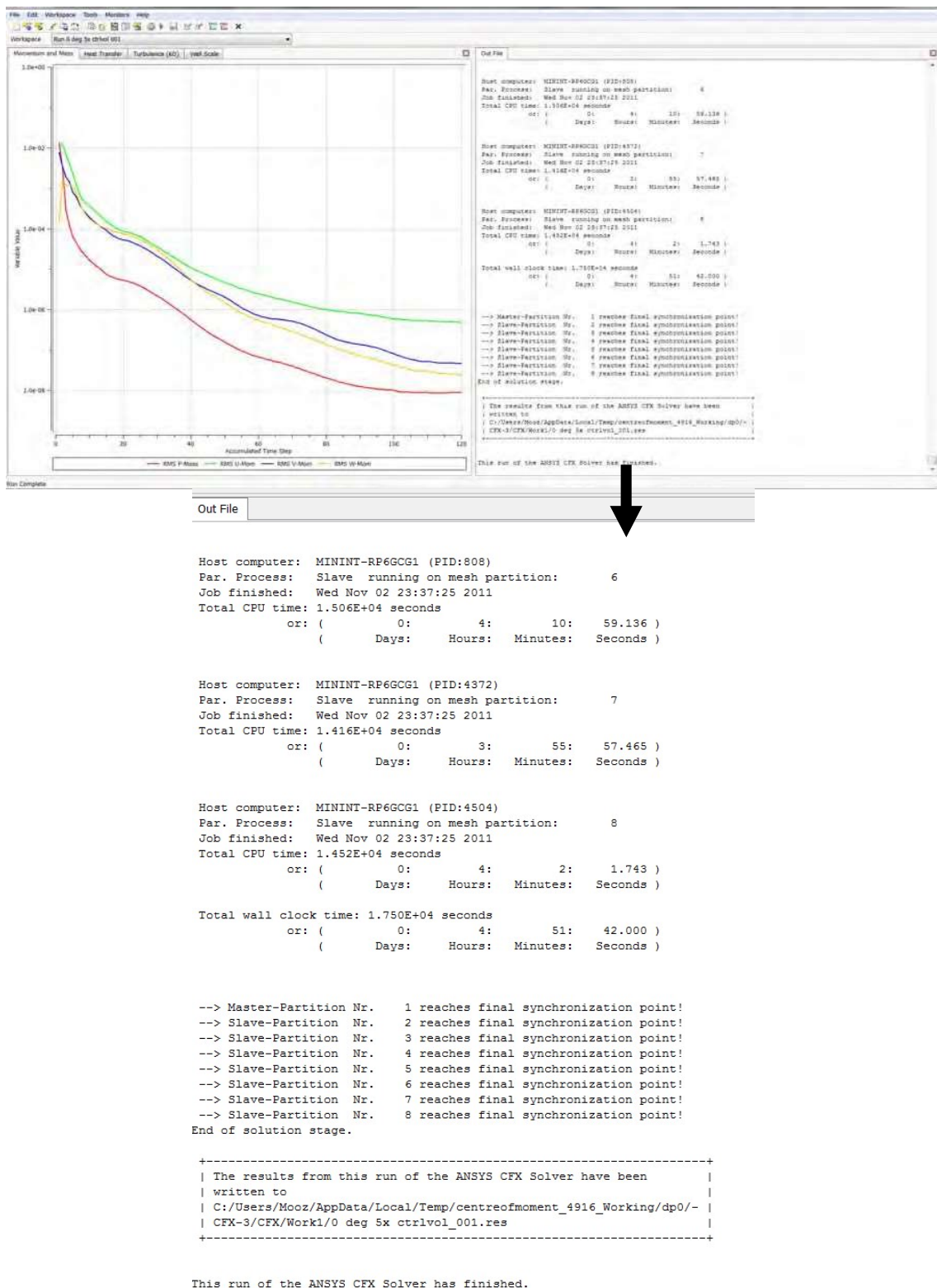


Figure 16. Display monitors.

## 4. DISPLAYING SIMULATION RESULTS

### a. Flow Field Display

CFX-Post is started by double clicking on the “Results” tab in the CFX workspace. In CFX-Post, the flow field around the missile model can be visualized and forces acting on the missile model can be calculated. In order to visualize the flow fields, a “slice” of the domain was created by the addition of planes in the XY and YZ directions. Figure 17 shows an example of the Mach number over the canard of the missile. The shocks off the nose and canard are clearly visible here.

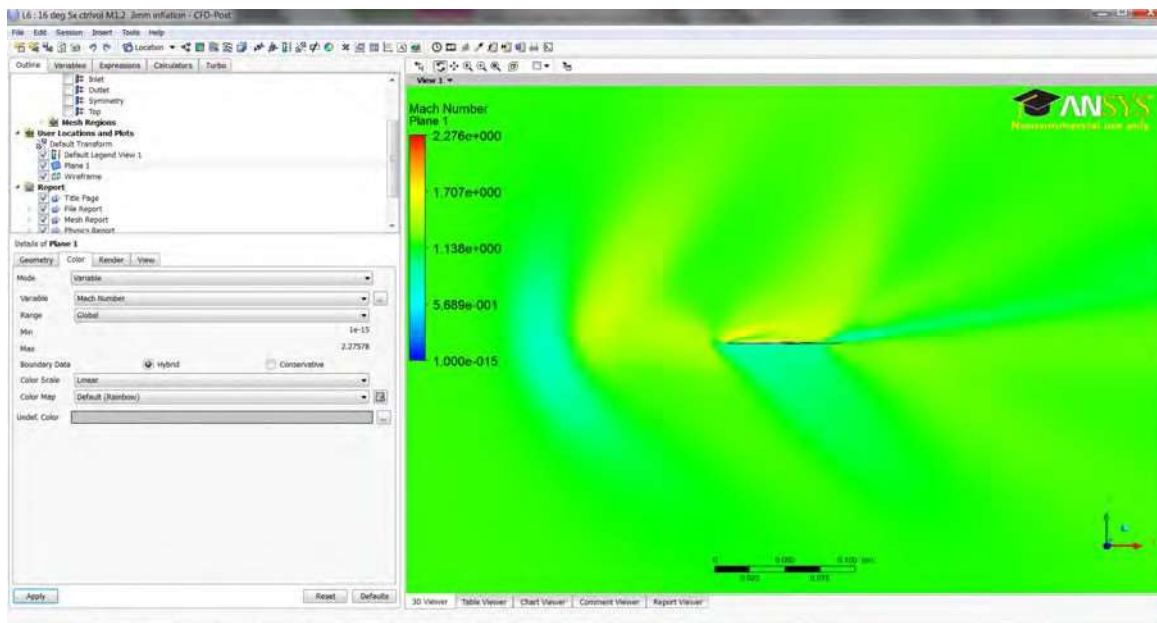


Figure 17. Mach number distribution over the canard.

The visualization of the vortices produced by the canard can also be shown in the YZ plane as shown in Figure 18.

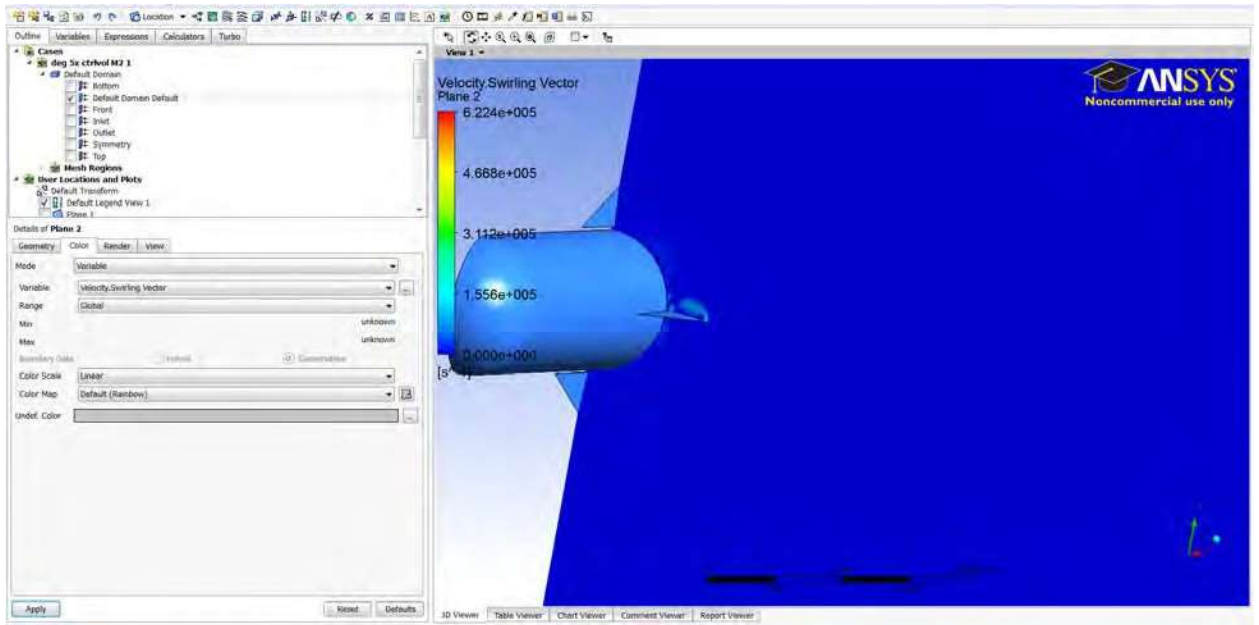


Figure 18. Vortex at canard leading edge.

### b. Function Calculator

The forces on the missile body can be calculated using the “Calculator” tab. The “Function Calculator” is used to calculate  $F_Y$ ,  $F_X$  and  $Torque_Z$ . The origin was placed at the Moment Reference on the missile body to facilitate the determination of Moment about the Moment Reference. In this method of simulation selected,  $F_Y$  and  $F_X$  correspond to the Normal force and Axial force and  $Torque_Z$  corresponds to the Moment about the Moment Reference. The average value of  $Y_{plus}$  can also be calculated. A screenshot of the Function Calculator is presented as Figure 19.

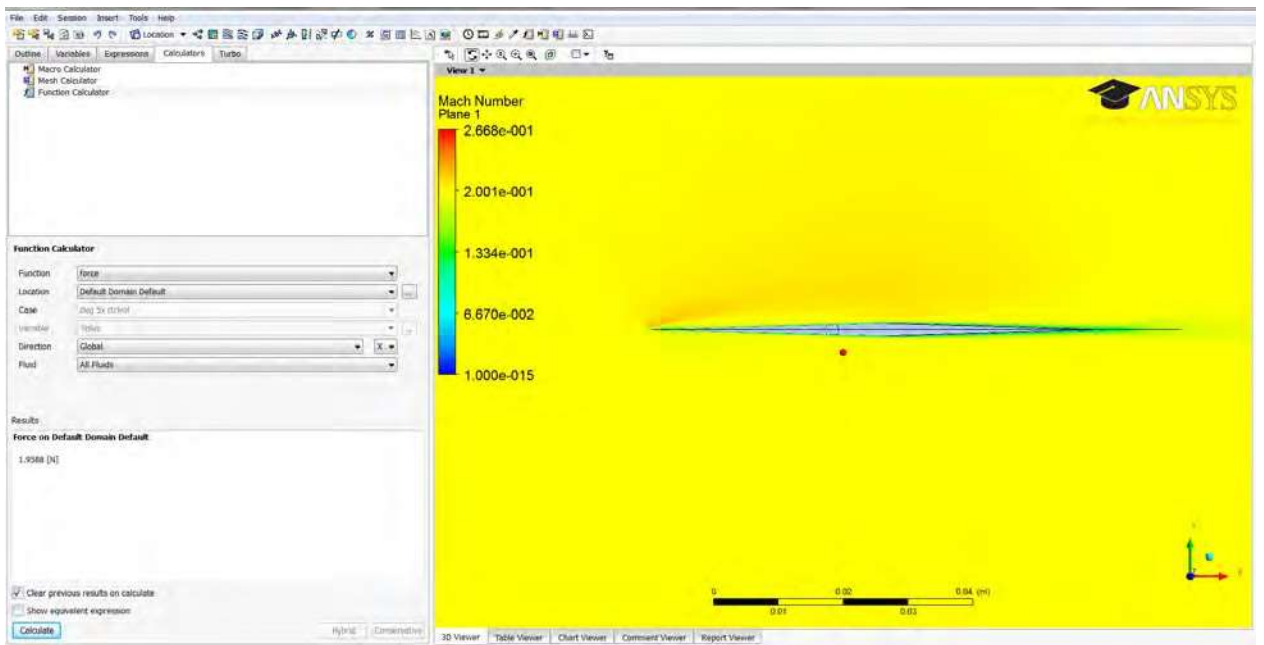


Figure 19. Function Calculator.

## The Project:

### INTRODUCTION:

#### A. CURRENT ANALYSIS TECHNIQUES

The use of computers to solve the Navier-Stokes equations was a major breakthrough for the study of aerodynamic problems. Before this, engineers and researchers were left with only using actual wind tunnel tests and approximations to determine the aerodynamic characteristics of flight objects. Currently, there are three primary methods that can be used for the study of flight vehicles. The most obvious and time honored is the use of a wind tunnel and an actual model of the vehicle to be tested. This would yield the most accurate aerodynamic characteristics of the vehicle. The second method uses software that contains a database of wind tunnel tests and other analytical data to predict the aerodynamic characteristics of the

flight vehicle. An example of such a program is Aeroprediction 2009 (AP09). The third method is to use Computational Fluid Dynamics (CFD) codes that solve the Navier-Stokes equations. Examples of such programs include NASA's OVERFLOW and commercially available codes like ANSYS-CFX.

## B. OVERVIEW OF SOLIDWORKS MODELLING

SolidWorks 2010 was the 3D CAD software that was used for this study. The software was used to create 3D drawings of the missile which was then imported into ANSYS-CFX for analysis. The Figure 1 shows the graphical interface of SolidWorks and a model of the missile created in this environment.

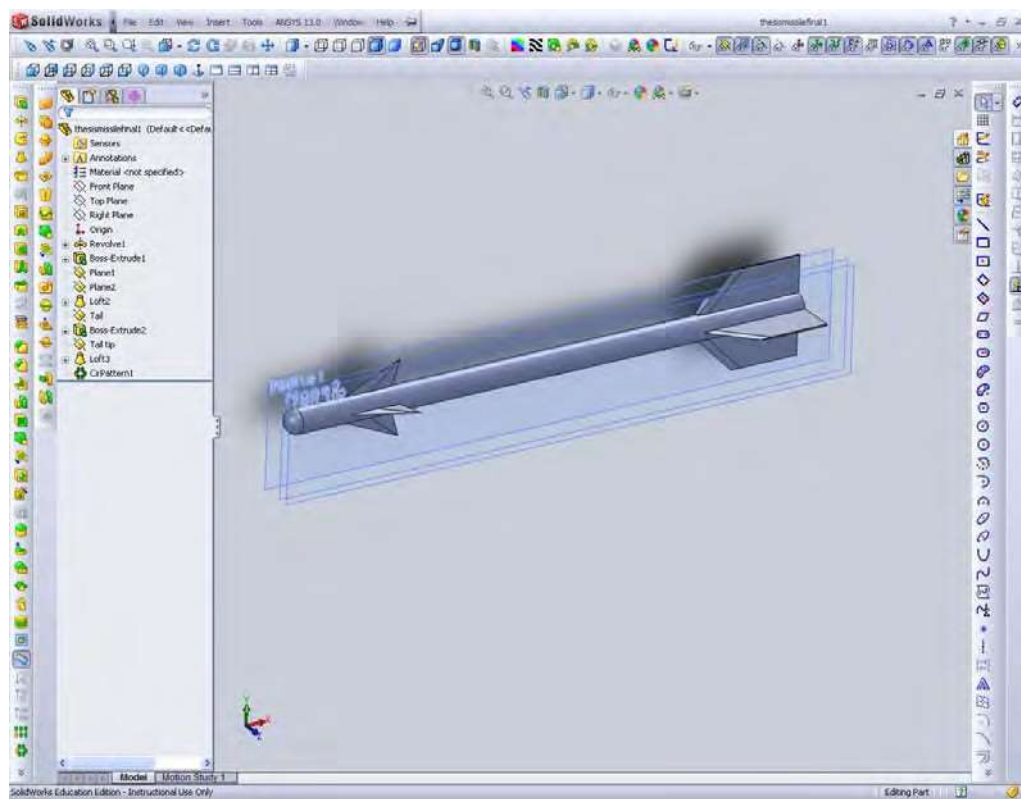


Figure 1. SolidWorks GUI.

## 1. MODEL SELECTION

The missile model chosen for this analysis consisted of a cylindrical body with triangular canards, a trapezoidal tail and a hemispherical nose. This model was chosen as wind tunnel data was readily available from NASA's Technical Memorandum by Graves and Fournier [1]. The report contained a schematic of the model used in the test as well as detailed data for  $C_M$ ,  $C_A$ ,  $C_N$  and  $C_L$  that was analyzed in this report. A detailed description of the steps to draw the model in SolidWorks is presented in Appendix A. The drawing of the missile and all dimensions were obtained from [2].

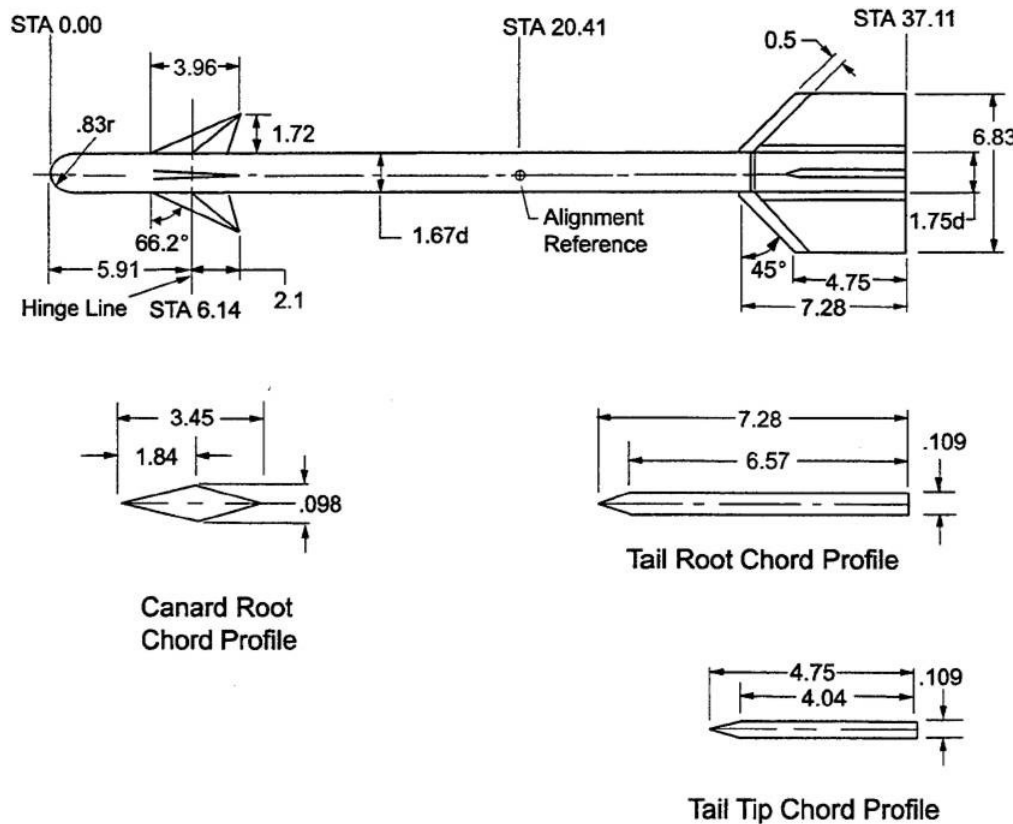


Figure 2. Missile drawing and dimensions. From [2].

## 2. ASSUMPTIONS MADE FOR THE MODEL

Some assumptions and approximations were made in the drawing of the model used. The assumptions made may result in differences in computed values using ANSYS- CFX. However, investigations into similar actual missiles (Figure 3) show the construction and attention to details with regard to drag reduction to be poor. These missiles often had parts that were not aerodynamically shaped like bolts which protrude out of the missile body. Examples of this can be seen in Figure 4 and Figure 5.



Figure 3. Picture of AIM-9 Sidewinder.



Figure 4. Picture depicting protruding bolts holding canard to hinge.



Figure 5. Picture depicting the method of attachment of tail fins to fuselage.

Hence, it was deduced that the designers of these missiles were not as concerned about drag and hence  $C_A$  as they were with lift and pitching moment. Therefore, it is reasonable for the analysis using ANSYS-CFX to state the following assumptions:

*a. Exclusion of Missile Hangers*

Actual missiles would have fixtures to attach the pylon holding them to the aircraft. These are removed for simplicity and are expected to have an effect on  $C_A$ .

*b. Inclusion of a Hinge to Hold Canards to Body*

Actual missiles would have a shaft protruding out of the missile body linking the actuator to the canard. It was observed that these shafts could be even wider than the canard itself on actual missiles. This can be seen in Figure 4. In this model however, they are represented by a shaft that is a fraction smaller in diameter compared to the canard at its thickest point. This approximation was expected to have an effect on  $C_A$ .

*c. Seating of the Tail Wings*

In this model, the seating for the tail wings was created by extruding the seat of the tail into the missile body. Appendix A illustrates this in Figure 67. In an actual missile, it was observed that the wings are clamped onto the body using support plates on both sides of the wings. This increased the diameter of the missile body and may have introduced

additional drag. The model simplified this by attaching the wing directly on to the missile body and omitting the plates that held the wing down (Figure 5). This was also expected to have an effect on  $C_A$ .

#### *d. Shape of the Wings and Canards*

In the wind tunnel tests, it was highlighted that the canards and tail wings had the pointed edges rounded off but to an unknown radius. In the CAD model, rounding off the pointed edges by anything more than 0.01 mm reduced the overall length of the canards and wings by a large amount. It was also found previously that ANSYS could handle these pointed edges. Hence, it was decided to not to round off these edges in the CAD model.

#### *e. Accuracy of Dimension Given in [1] and [2].*

After the model was drawn in Solidworks, it was discovered that the canard leading edge sweep angle of  $66.2^\circ$  was not achievable if all other dimensions were followed. Measurement of the 3D model yielded a sweep angle of  $66.52^\circ$  instead. This was the value used in this simulation.

### **C. OVERVIEW OF ANSYS CFX**

ANSYS-CFX is one of the two CFD codes that are part of the ANSYS suite of programs, the other CFD code being FLUENT. The primary difference in the two codes is ANSYS-CFX solver uses finite element (cell vertex numerics) to discretize the domain whereas ANSYS- FLUENT uses

finite volume elements (cell-centered numerics). In this study, ANSYS-CFX is used. The version of ANSYS used is ANSYS Release 13.0.

ANSYS-CFX is integrated into ANSYS Workbench Environment, which offers users a graphical interface for which to access all the functions within ANSYS with simple drag-and-drop operations. ANSYS-CFX itself consists of five modules, Geometry (DesignModeler), Meshing, Setup (CFX-Pre), Solution (CFX Solver) and Results (CFX Post). Figure 6 shows the ANSYS Workbench GUI and the five modules of CFX.

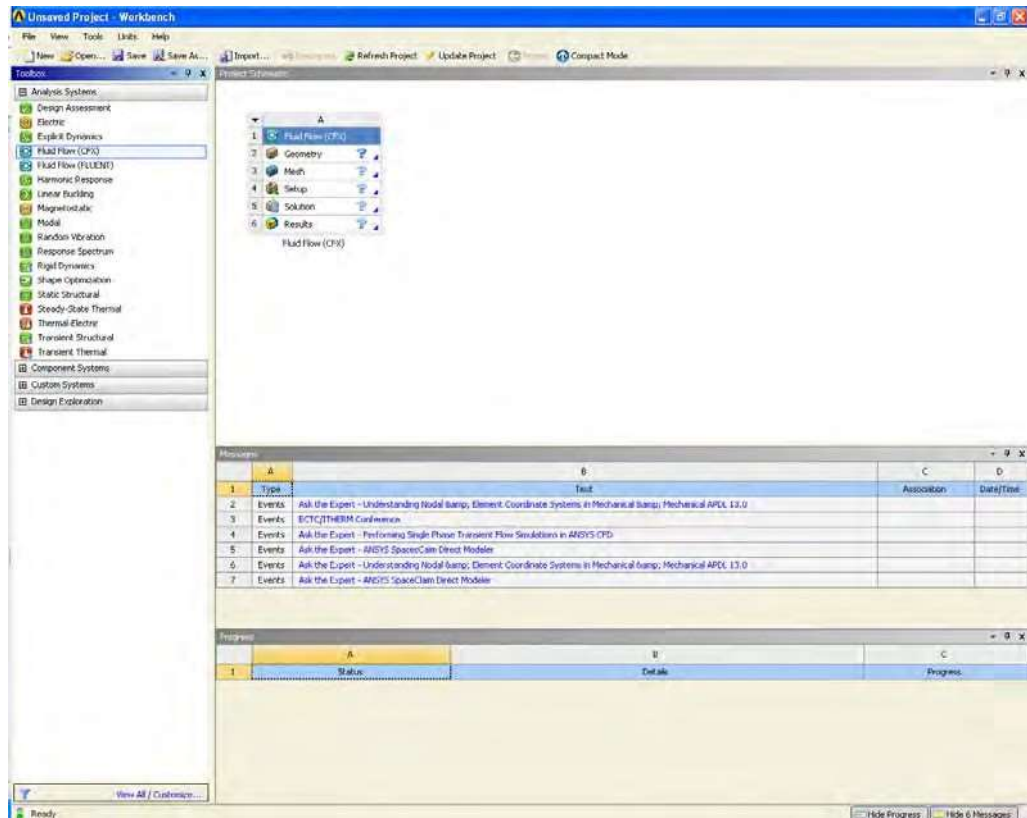


Figure 6. ANSYS GUI.

## FUTURE SCOPE:

In order to increase the capabilities of modern missiles and missile defense systems, the global defence industry is investing significantly in research and development which has led to the development of technologies to enhance the speed, accuracy and destructive power of missiles.

Current innovations are oriented towards increasing speed with hypersonic missiles, shooting down missiles in mid-air with interceptors, enhancing anti-aircraft carrier capabilities, increasing payload capacity, facilitating navigation and introducing stealth capabilities.

### **Smokeless missiles to prevent target back to fire**

Charming Defence of the UK has developed a multiple-effects rocket system (MERS) which can fire missiles without emitting any smoke. This benefits the person firing the missile, as the enemy will not be able to judge the place from where the missiles are being fired, reducing the risk of enemy attack.

MERS has a new ground target smoke capability, in which the smoke payload can be fired at an angle along the ground to mark a target for directing fire or aerial attack.

Also, the advanced propellant used enables the payload to travel at a greater speed, making it more stable and accurate in flight, particularly in windy conditions.

The system is designed to reach targets at distances of 300-600 metres without varying the length of the missile packing. Chemring also has plans to introduce MERS with a range of 1,000 metres.

### **Anti-aircraft-carrier missile capable of being launched from mobile launch platforms**

The Taiwanese defence ministry has launched a programme to develop an anti-aircraft-carrier missile capable of being launched from mobile platforms.

Perceiving a threat from China's newly launched aircraft carrier, the Taiwanese Government is developing these missiles to ensure the country's missiles systems are less prone to being hit by enemy attacks. The missiles

being developed are expected to have a long range and will carry a heavy warhead.

### **Laser defence systems which blind missiles during flight**

The University of Michigan in the US has developed a novel laser technology capable of blinding in-flight heat-seeking missiles.

The laser technology protects helicopters by using inexpensive telecommunications fiber optics to produce sturdy and portable mid-infrared supercontinuum lasers.

These lasers produce a focused beam of light from a much broader range of wavelengths which can mimic the electromagnetic signature of the helicopter and confuse the missile.

The Defense Advanced Research Projects Agency (DARPA) has granted US\$1 million to build a second-generation prototype of the technology.

Boeing has also successfully completed the initial design of an electron laser weapon which generates an intense laser light emission that can disable or destroy targets when a beam of high-energy electrons are passed through a series of powerful magnetic fields.

### **New materials to make existing weapons more powerful**

The US Office of Naval Research (ONR) has been researching and developing high-density reactive material (HDRM) for many years and has begun a series of tests on weapons made using the material.

The material is made by combining several metals and has the potential to make existing weapons more accurate and powerful without changing the explosives used.

Munitions designed using HDRM integrate the casing with the warhead explosives, making them more deadly. This is particularly effective for fragmenting warheads, which release additional chemical energy after impact, thereby increasing lethality.

### **High speed missiles with better kinetic performance in demand**

A consortium comprising some of the key European spenders including the UK, Germany, Italy, Spain, France and Sweden is developing high-speed AAMs to be installed on combat aircraft.

These missiles are still in their development stage and are expected to be capable of travelling at Mach 4, making evasive action difficult. The missiles are expected to have a greater range and will be guided by radar systems to be able to chase and destroy a moving target.

They are expected to have kinematic performance which will be three to six times greater than the AAMs currently being used by the global defense ministries. The missile uses a throttleable ducted rocket (TDR) propulsion system which enables long range and high average speed.

India is also developing hypersonic cruise missiles with a maximum speed of 6,000 kilometers an hour to increase its aerial fast-strike capability. The hypersonic cruise missile will be developed on the basis of the existing BrahMos supersonic cruise missile version with technical support from Russia. They are designed with a range of more than 300 kilometers and have a high target-penetration capability.

The US Army also wants missile technology which can enable them to attack anywhere on earth within an hour. The US Arclight Program is investigating a very-long-range weapon, incorporating a hypersonic glider.

### **Missile defence systems capable of intercepting missiles in space under development**

Defense ministries around the world are developing a missile defense system capable of intercepting enemy missiles in the highest layer of the atmosphere and in outer space.

These defense systems detect an incoming missile and destroy the missile in the upper layers of the atmosphere.

A number of these missile defense systems are being developed: China is developing a missile defense system which uses kinetic energy to intercept ballistic missiles and other aerospace vehicles within the upper atmosphere at altitudes greater than 80 kilometers.

India has also developed an advanced version of its indigenous two-tier BMD system which is capable of intercepting enemy missiles at exo-atmospheric altitudes of 150 kilometers and endo-atmospheric heights of 80 kilometers.

The Israeli Defense Force (IDF) has deployed a rudimentary version of this system, the Iron Dome, which is capable of intercepting short-range rockets

with moderate small warheads, fired from a distance of 4.5-70 kilometers, and can protect an area as large as ten square kilometers against rockets and mortar shells.

## Results and Discussions:

Parabolic Nose Profile

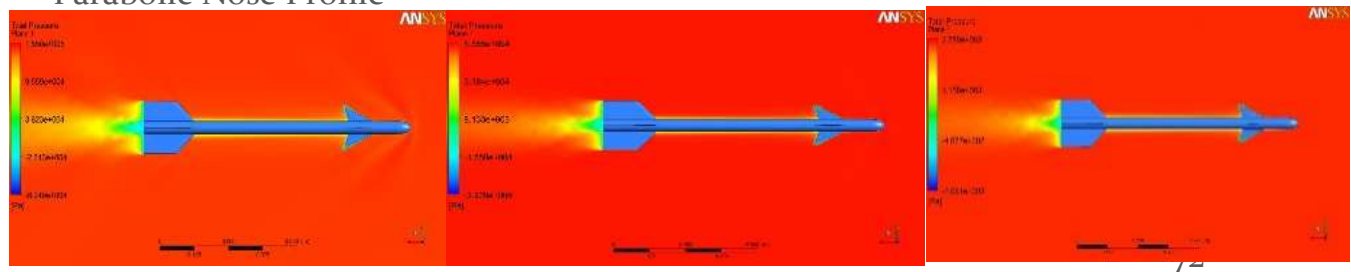


Figure 1 a

Figure 1 b

Figure 1 c

## 1.2 Total Pressure Plot

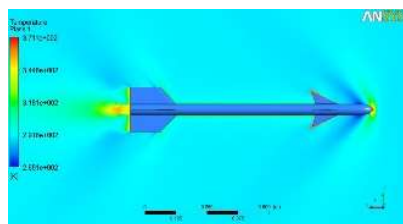


Figure 2 a

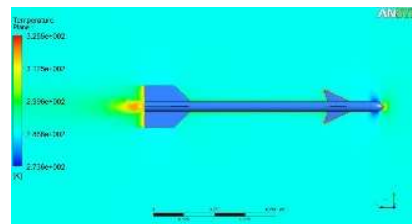


Figure 2 b

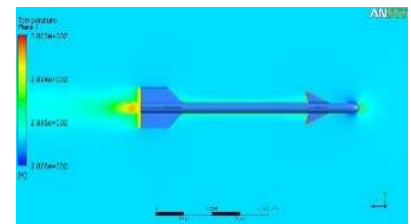
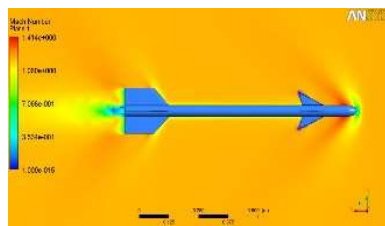
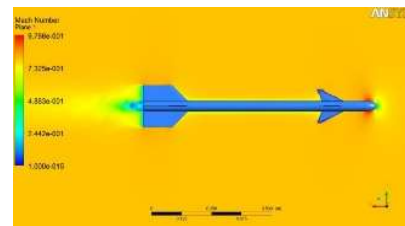


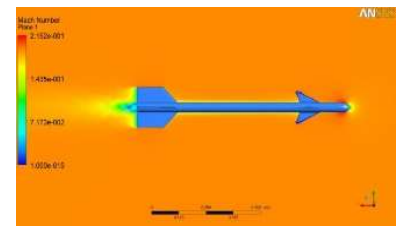
Figure 2 c



1.2 Mach Plot



0.8 Mach Plot



0.2 Mach Plot

The plots on Parabolic Nose Profile signify variation of Total Pressure, Temperature and Mach along the length of missile Body.

Higher temperature at surface is inevitable at higher Mach number which is correctly depicted by the Temperature contours.

The pressure variation depicted by Mach plot shows the low pressure region formed at Tip due to stagnation, and consequent high pressure areas.

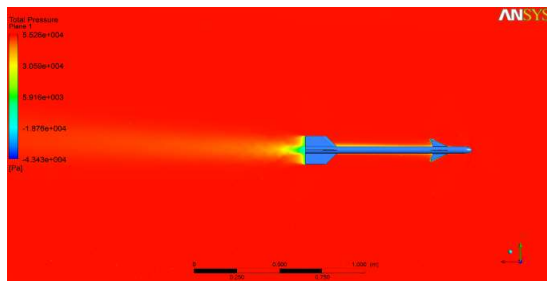


Fig i(a)

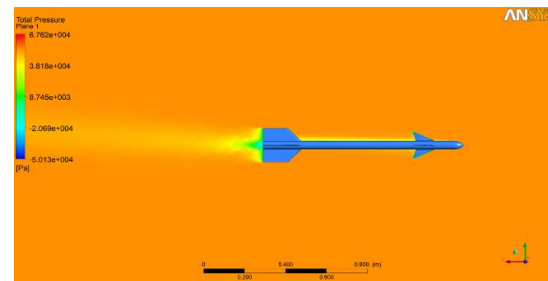


Fig i(b)

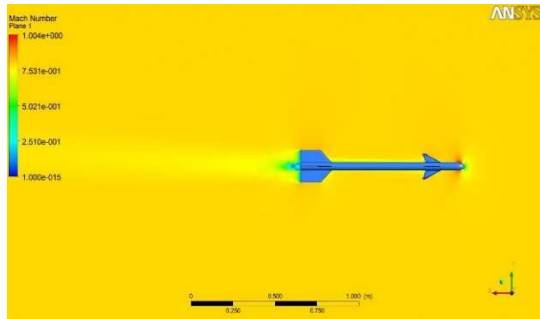


Fig ii(a)

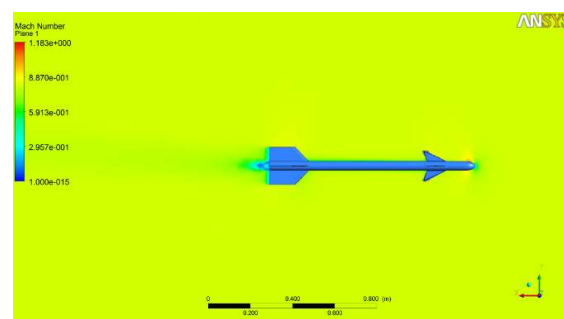
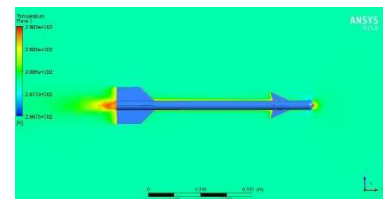


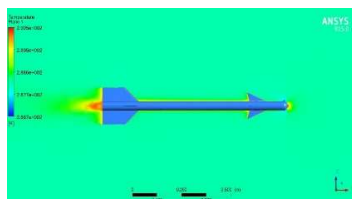
Fig ii(b)

Fig i(a);(b);ii(a);(b) represent Total Pressure and Mach Plot at 4 and 6 AOA respectively

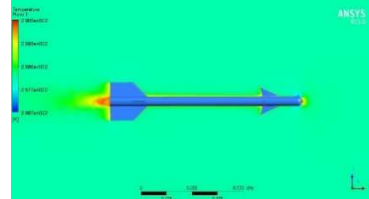
#### Hemispherical Nose Profile



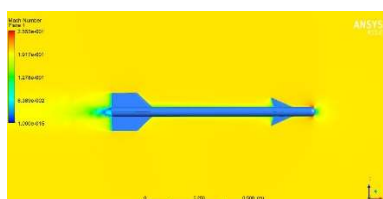
1.2 Temperature Plot



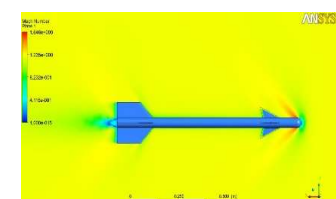
0.8 Temperature Plot



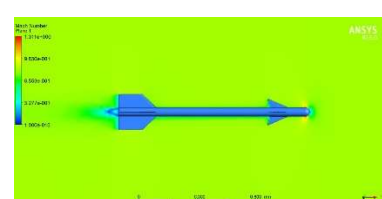
0.2 Temperature Plot



1.2 Mach Plot



0.8 Mach Plot



0.2 Mach Plot

## ELLIPSOID NOSE PROFILE (1.2 Mach)

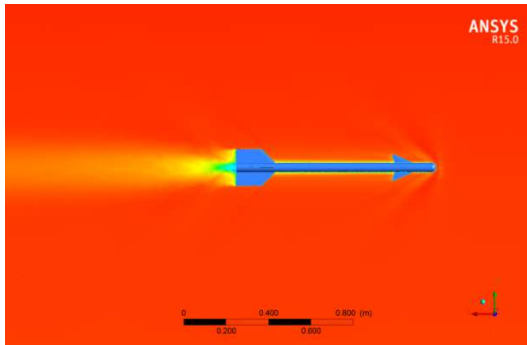


Fig 1(a)

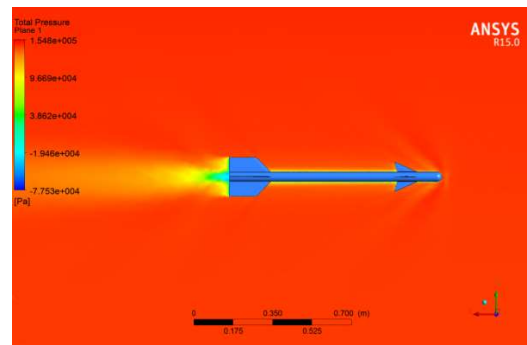


Fig 1(b)

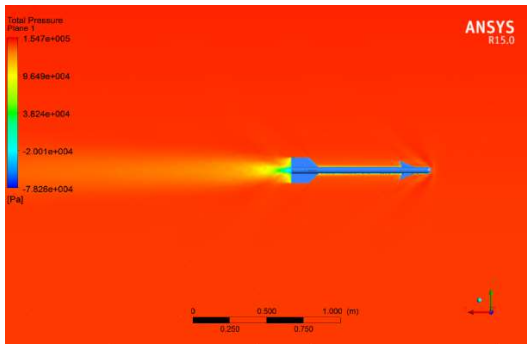


Fig 1(c)

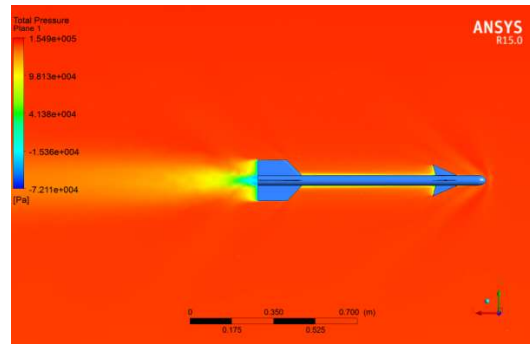


Fig 1(d)

Fig 1(a);(b);(c);(d) represent Total Pressure at Eccentricities 0.2;0.4;0.6 and 0.8 respectively

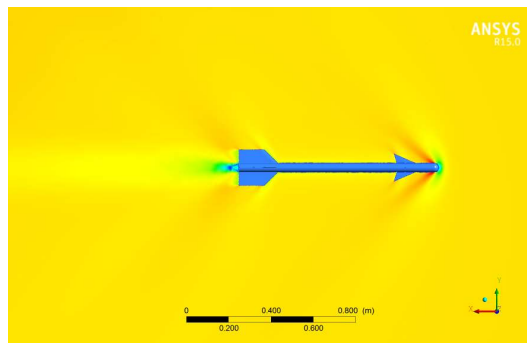


Fig 2(a)

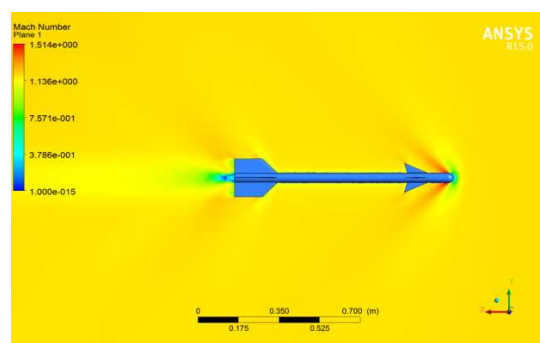


Fig 2(b)

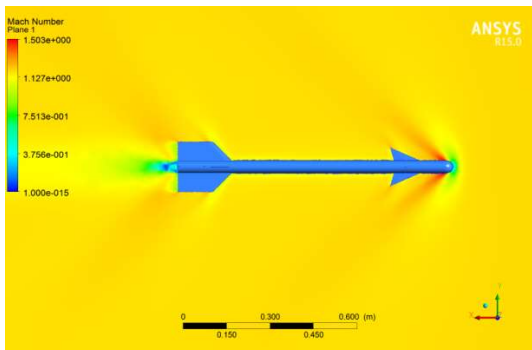


Fig 2(c)

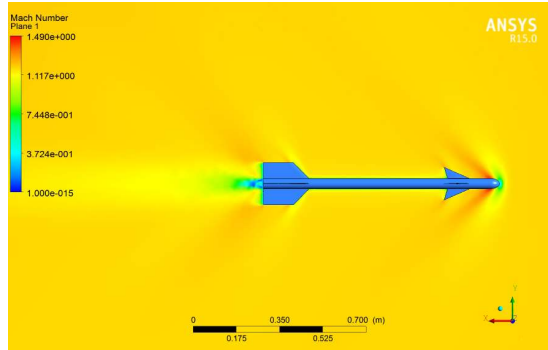


Fig 2(d)

Fig 2(a);(b);(c);(d) represent Mach Plot at Eccentricities 0.2;0.4;0.6 and 0.8 respectively

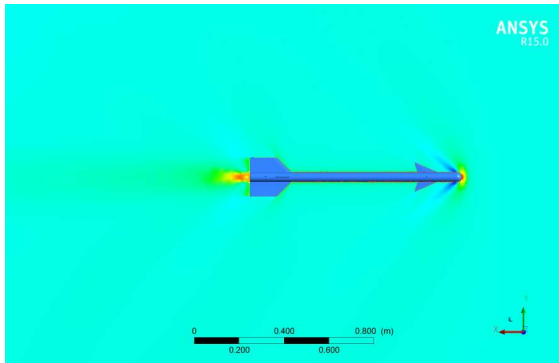


Fig 3(a)

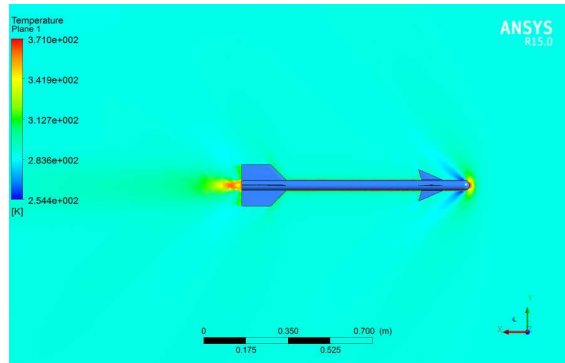


Fig 3(b)

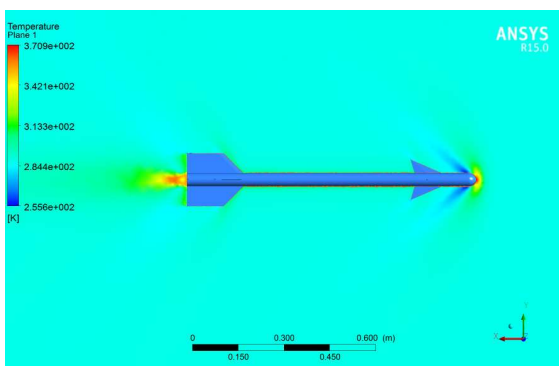


Fig 3(c)

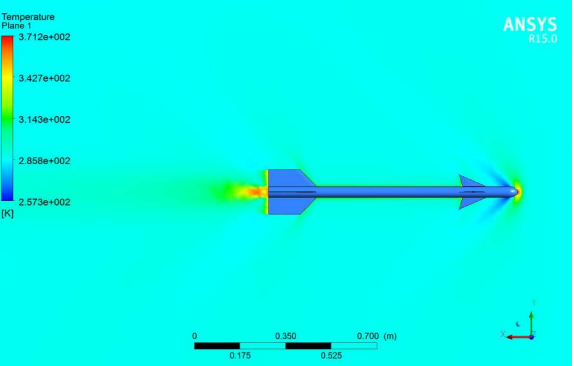
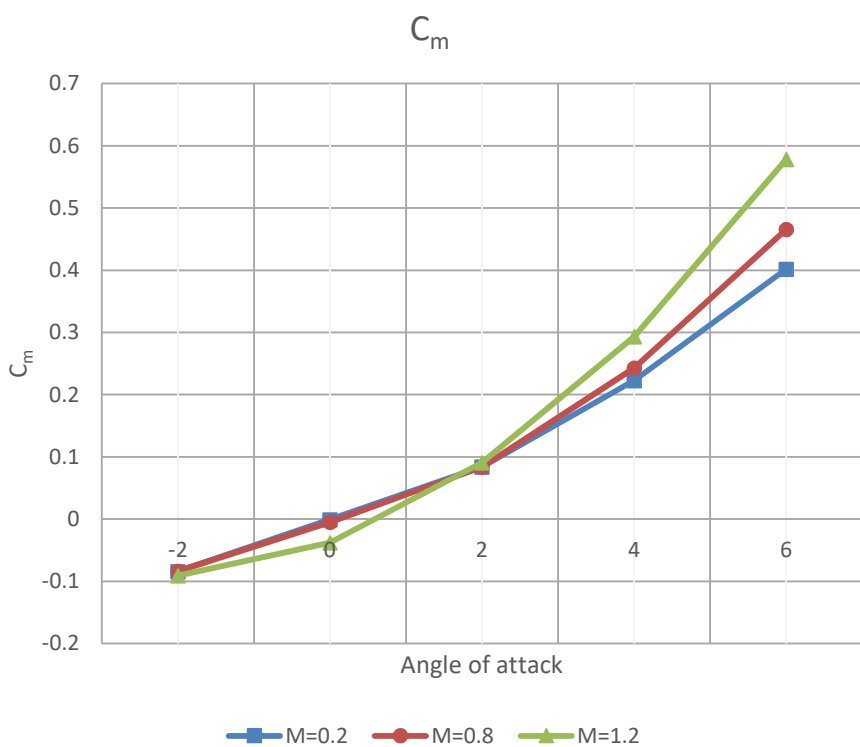
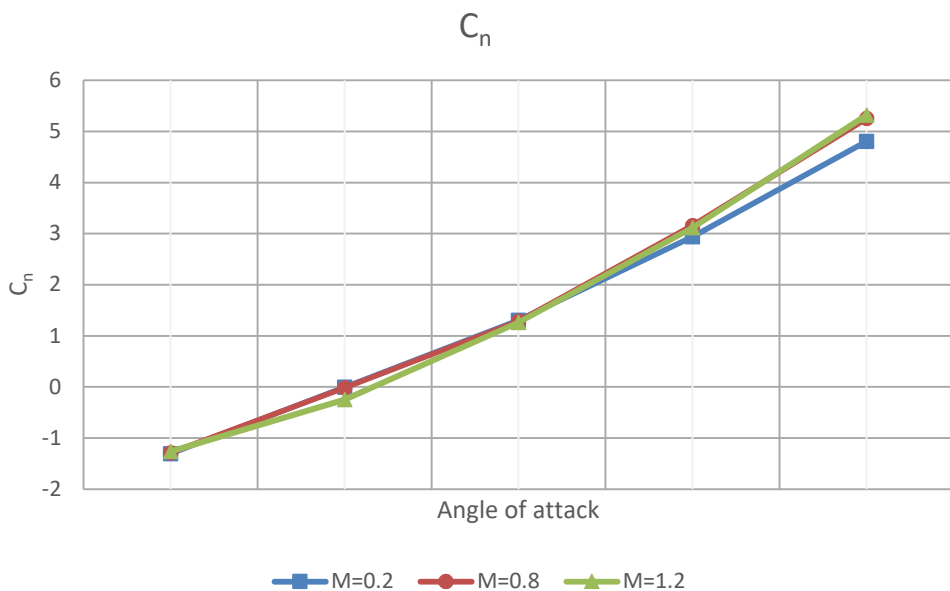
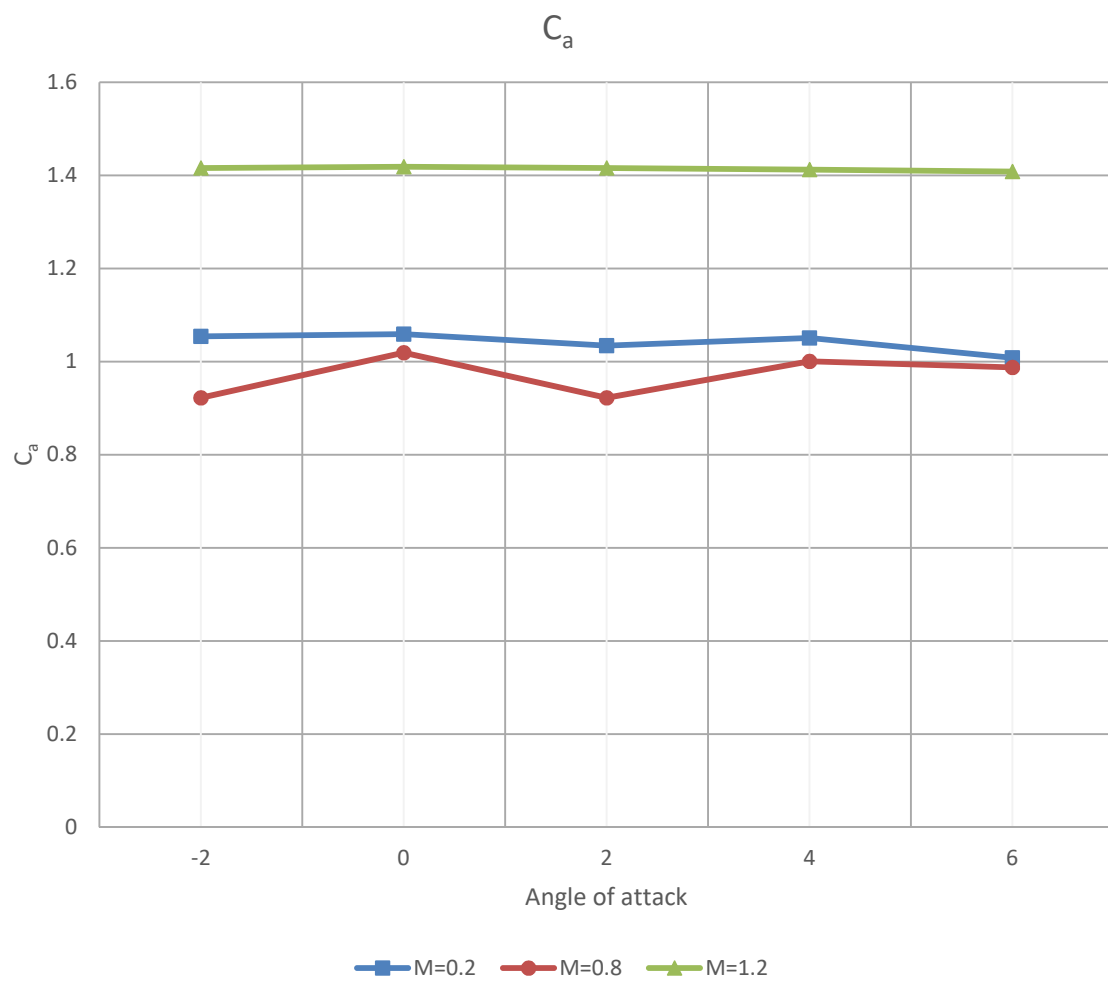


Fig 3(d)

Fig 3(a);(b);(c);(d) represent Temperature Plots at Eccentricities 0.2;0.4;0.6 and 0.8 respectively

Comparison of Hemispherical and Parabolic Nose Profiles for different Coefficients:





## Conclusions and summary:

An ANSYS-CFX computation of the flow over a canard missile configuration was completed for Mach number of 0.2, 0.8 and 1.2 and their results compared against experimental data obtained from wind tunnel test and data obtained from AP09. The results show good agreement at Mach number of 0.2, 0.8 and 1.2 for  $C_A$ ,  $C_N$ , and  $C_L$ . Results for drag show less agreement and are probably due to the turbulence models used. Further research and improvements with regard to turbulence models must be made in order to improve the computational codes and accuracy of predicting flow behavior. Considerable time and computational power was also expended in the use of ANSYS-CFX to complete the simulations for this research.

The results show that boundary layer separation can be postponed by the shape of the nose of missile. The idea here is to get the static pressure at the base of the fore body to be as large as possible. This will give the greatest critical Mach number and the least adverse pressure gradient over the cylindrical after body. Although vortices cannot be avoided, they can be mitigated by using the best nose cone shapes that can produce high critical Mach numbers with respect to ambient pressure.

Here Ellipsoid nose gives highest critical Mach numbers and lowest flow separation. It was also observed that Parabolic Nose gives higher critical Mach numbers than hemispherical Nose Profiles at subsonic speeds. Whereas results of parabolic and hemispherical are similar at near supersonic speeds.

At lower angle of attacks parabolic profiled noses gives maximum drag and Axial force coefficients. But at higher angle of attacks hemispherical nose have highest drag.

At higher angles of attack ellipsoidal nose has lowest pitching moments (Pitching Moment Coefficients) and hence highest stability. Whereas hemispherical has lowest stability at high angle of attacks.

## REFERENCES

- [1] Hong Chan Wee, Maximillian Platzer and Garth Hobson, “Aerodynamic Analysis of a Canard Missile using Ansys CFX.” Naval Postgraduate School, Monterey, California, Dec 2011
- [2] E. B. Graves, and R. H. Fournier, “Stability and control characteristics at Mach numbers from 0.20 to 4.63 of a cruciform air-to-air missile with triangular canard controls and a trapezoidal wing.” National Aeronautics and Space Administration,  
Langley Research Center, Hampton, VA, NASA TM X-3070, July 1974.
- [3] F. G. Moore, T. C. Hymer, C. Downs and L. Y. Moore, “The 2002 Version of the NSWC Aeroprediction Code: Part 1 – Summary of New Theoretical Methodology,” Dahlgren Division Naval Surface Warfare Centre, Dahlgren, VA, NSWCDD/TR-01/108, Mar 2002.
- [4] A Sanjay Verma, G Sai Sathyanarayana and Sandeep J, “CFD Analysis of Various Nose Profiles.” MRCET, Secunderabad.
- [5] B. Tyler Brooker, John Baker, Kwith A. Williams, “Experimental Study on the Effects of Nose Geometry on Drag over Axisymmetric Bodies in Supersonic Flow.” University of Alabama, Alabama.
- [6] Tan, Wei Chieh, “Aerodynamic validation of emerging projectile and missile configurations.” Naval Postgraduate School, Moterey, CA
- [7] Z. Eghlima and K.Masou, “Drag Reduction for spike and counterflow jett on blunt body at high Mach Nuber flow.” Amirkabir University of Technology, Tehran, Iran